The experimental study of electron–phonon scattering in metals

V F GANTMAKHER

Institute of Solid State Physics, Academy of Sciences of the USSR,
Chernogolovka, USSR

Abstract

The review is devoted to low temperature methods of the study of electron scattering on phonons in metals. The basic emphasis is put on those experiments or those aspects of experiments which are governed by or can yield information about the electron–phonon scattering anisotropy, ie the dependence of scattering probability on the electron position on the fermi surface.

This review was completed in November 1972.

Contents

1. Introduction

Over the last twenty years the work of metal physicists has centred on the study of the effect of the crystal lattice on electronic spectra. A wide field of study developed and even acquired a special name—fermiology. The development of this field has been outstandingly successful. The fermi surfaces of most metals have now been studied in detail and are known very accurately. For example, the deviations from sphericity of the fermi surface of sodium, which are less than 0·1%, have been measured and plotted on a stereographic projection. In parallel with this, the genesis of the electronic spectrum has also become clear, at least for non-transition metals, as a result of the development of the theory of pseudopotentials. The successes of fermiology have to a large extent been summarized in the book *The Physics of Metals*, edited by Ziman (1969).

The fantastic shapes of fermi surfaces, which have sometimes excited the admiration of artists and sculptors, are determined basically by the fact that the electron moves in the periodic potential of the crystal lattice. However, this is by no means the only effect on the electrons of the ideal crystal lattice. Electrons also interact with lattice vibrations, ie phonons, and the electron–phonon interaction determines many of the basic properties of metals. Perhaps the most important is superconductivity, which is due to an indirect electron–electron interaction which takes place through phonons. Interactions with phonons also change the effective mass of an electron; as a rule electrons which are dressed in a 'phonon cloud' become heavier. For example, the effective mass in sodium is $m^* = 1{\cdot}24m_0$, where m_0 is the mass of a free electron, and in lead and mercury electrons become heavier by a factor of 2·5 as a result of interaction with phonons. Another aspect of this interaction, the absorption of phonons by electrons, is closely related to ultrasonic attenuation in metals, since sound is a directed flux of these phonons. At the same time the scattering of electrons by phonons limits the mean free path of current carriers and this affects all the kinetic properties of metals.

All these effects are now intensively studied in many laboratories around the world. Indeed, it is no exaggeration to say that this field is the centre of gravity of research in the physics of metals. Moreover, this research now has a qualitatively new foundation, based on known fermi surfaces and known phonon spectra.

The present review is devoted to one aspect of this field. We shall discuss the experimental methods for the study of the scattering of electrons by phonons and the experimental results at present available. The main emphasis will be placed on phenomena which are due to, or can give information on, the anisotropy of electron–phonon scattering and its dependence on the position of the electron on the fermi surface. In general, studies of scattering make use of methods developed in fermiology which pick out particular groups of conduction electrons (cyclotron resonance, size effects, ultrasonic attenuation in a magnetic field, etc). However, the desire to obtain from 'old' methods new information, not about the spectrum of electrons but about their lifetimes, makes one re-examine critically the possibilities of these methods.

2. Scattering probability

2.1. General expressions

2.1.1. Conservation laws and the matrix element. The scattering of electrons by phonons is described in the language of particle collisions; an electron at some point in its trajectory either absorbs or emits a phonon (figure 1). This process must

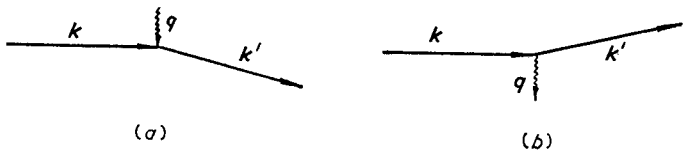

Figure 1. Schematic representation of (*a*) absorption and (*b*) emission of a phonon by an electron with wave vector $\boldsymbol{k}$.

obey the conservation laws for energy

$$E_{k'} = E_k \pm \epsilon \tag{1}$$

and quasimomentum

$$\boldsymbol{k}' = \boldsymbol{k} \pm \boldsymbol{q} + \boldsymbol{K}. \tag{2}$$

($E_k, E_{k'}, \boldsymbol{k}, \boldsymbol{k}'$ are respectively the energies and wave vectors of the electron before and after the scattering; $\boldsymbol{q}$ and ϵ are the wave vector and energy of the phonon; $\boldsymbol{K}$ is any reciprocal lattice vector; the upper sign corresponds to phonon absorption and the lower to phonon emission.) The probability ν_q, that scattering by a phonon with wave vector $\boldsymbol{q}$ satisfying (1) and (2) in fact takes place, depends on the square of the interaction matrix element $M^2(\boldsymbol{k}, \boldsymbol{q})$, on the number of phonons ϕ_ϵ in state $\boldsymbol{q}$ and on the probability that the electron state with momentum $\boldsymbol{k}'$ is empty:

$$\nu_q(\boldsymbol{k}) = \frac{2\pi}{\hbar} M^2(\boldsymbol{k}, \boldsymbol{q}) \left[\Phi_+\left(\frac{E}{T}, \frac{\epsilon}{T}\right) \delta(E_{k'} - E_k - \epsilon) + \Phi_-\left(\frac{E}{T}, \frac{\epsilon}{T}\right) \delta(E_{k'} - E_k + \epsilon) \right] \tag{3}$$

(here $\Phi_+ = \phi_\epsilon(1 - f_{E+\epsilon})$; $\Phi_- = (\phi_\epsilon + 1)(1 - f_{E-\epsilon})$; f_E is the electron distribution function; the δ-functions ensure conservation of energy and the temperature T is expressed in ergs, ie Boltzmann's constant is taken as unity). The total probability for the scattering of an electron by phonons is given by

$$\nu(k) = \frac{1}{(2\pi)^3} \int \nu_q(\boldsymbol{k})\, \mathrm{d}^3 q. \tag{4}$$

The quantity $\nu(\boldsymbol{k})$ is also called the total collision frequency of an electron with phonons.

Since we are concerned with low temperatures, we shall deal below only with acoustic phonons. We use a model in which $M^2(\boldsymbol{k}, \boldsymbol{q})$ has the form (Ziman 1960, chap 5)

$$M^2(\boldsymbol{k}, \boldsymbol{q}) = \hbar q \Delta^2 / 2\mu s \tag{5}$$

where Δ is the deformation potential; s the velocity of sound; and μ is the density of the crystal. The use of (5) presupposes a whole series of assumptions and simplifications. The most important of these is that the deformation potential is really a tensor $\tilde{\boldsymbol{\Delta}}$ and appears in the matrix element in the form $\Delta_{ij}(\partial u_i/\partial x_j) \sim (\boldsymbol{e}\tilde{\boldsymbol{\Delta}}\boldsymbol{q})$, where $\boldsymbol{u}$ is the deformation vector and $\boldsymbol{e}$ is the phonon polarization vector (Akhiezer 1938). We replace $\tilde{\boldsymbol{\Delta}}$ by a scalar and simultaneously take some average value of the velocity of sound s. The factors less than unity, such as the square of the cosine

of the angle between $\boldsymbol{e}$ and $\tilde{\Delta}\boldsymbol{q}$, then drop out of $M^2(\boldsymbol{k},\boldsymbol{q})$; and also we integrate only over one of the three acoustic branches, since $M^2 = 0$ for a scalar Δ and purely transverse polarizations.

This all shows that one should not attach great significance to the numerical coefficients in the expressions which are derived below, using this matrix element. We shall, however, always write out these coefficients because they are useful in comparisons between different situations.

2.1.2. Region of integration. We now turn to the expression in square brackets in (3). We shall be concerned only with degenerate fermi systems of electrons with fermi energies $E_f \gg T$, with velocities at the fermi surface $\boldsymbol{v} = \hbar^{-1}\nabla_k E$, which are much greater than s, the velocity of sound. This latter condition means that in a collision with a phonon the electron displacement perpendicular to the constant energy

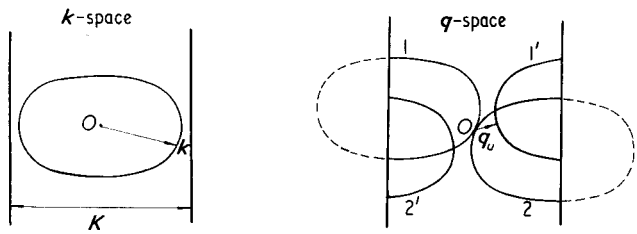

Figure 2. (*a*) Fermi surface $F(\boldsymbol{k}) = 0$ in $\boldsymbol{k}$ space; $\boldsymbol{K}$ is a reciprocal lattice vector. (*b*) Surfaces in $\boldsymbol{q}$ space defining the wave vectors of phonons that can be absorbed (1 and 1′), or emitted (2 and 2′), by an electron in state $\boldsymbol{k}$; $\boldsymbol{q}_u$ is the minimum wave vector of a phonon which can be absorbed or emitted by an electron $\boldsymbol{k}$ in an Umklapp process ($\boldsymbol{K} \neq 0$ in equation (2)).

surface $\Delta k_\perp \approx \Delta E/|\nabla E| \approx qs/v$ is much less than the displacement parallel to it $\Delta k_\parallel \approx q$, and hence it may be considered that the scattered electron remains on the same constant energy surface, ie that the scattering is elastic. Thus, in the integration in (4), the δ-functions pick out values of $\boldsymbol{q}$ which leave the electron on practically the same constant energy surface, when it is scattered with either the absorption or emission of a phonon. Moreover, if some particular value of $\boldsymbol{q}$ reduces to zero the argument of the first δ-function in (3), then the value $-\boldsymbol{q}$ reduces the argument of the second δ-function to zero, since a transition by an electron from state $\boldsymbol{k}$ to state $\boldsymbol{k}'$ can take place either by the absorption of a phonon with wave vector $\boldsymbol{q}$ or by the emission of a phonon with wave vector $-\boldsymbol{q}$. If the constant energy surface is described by the expression $F(\boldsymbol{k}) = 0$, then for an electron with initial wave vector $\boldsymbol{k}$ the first δ-function has zero argument on the surface $F(\boldsymbol{q}+\boldsymbol{k}) = 0$ in $\boldsymbol{q}$ space (the initial surface, displaced by a vector $-\boldsymbol{k}$), whilst the second has zero argument on the surface $F(-\boldsymbol{q}+\boldsymbol{k}) = 0$ (the initial surface, inverted through the origin, and then displaced by a vector $\boldsymbol{k}$). These two surfaces touch at the origin (see figure 2).

If these surfaces intersect the Brillouin zone boundaries, this means that some of the collisions take place by Umklapp processes ($\boldsymbol{K} \neq 0$ in (2)). If the Brillouin zone boundaries do not intersect the surfaces $F(\pm\boldsymbol{q}+\boldsymbol{k}) = 0$, then we always have $\boldsymbol{K} = 0$ in (2).

Whether Umklapp processes take place or not is important from two points of view. First, these collisions are necessary to produce dissipation of the momentum

of the electron–phonon system. Secondly, by means of Umklapp processes, ie transitions involving a reciprocal lattice vector (see figure 2), some parts of the surfaces $F(\pm \boldsymbol{q}+\boldsymbol{k}) = 0$ can lie much closer to the origin in the phonon-wave vector space, and this affects the temperature dependence of the quantity $\nu(\boldsymbol{k})$. The temperature T_u at which Umklapp processes begin to make a contribution to $\nu(\boldsymbol{k})$ comparable with that from normal processes is given, in order of magnitude, by $T_u \approx \hbar q_u s$, where the meaning of the minimum Umklapp wave vector $\boldsymbol{q}_u$ for a given k is clear from figure 2.

Since the phonon spectrum has a centre of symmetry, $\epsilon(\boldsymbol{q}) = \epsilon(-\boldsymbol{q})$, the surfaces of integration over $\boldsymbol{q}_u$ are identical for the two terms in (3) and we can write

$$\nu(\boldsymbol{k}) = \frac{1}{(2\pi)^2\hbar}\int \frac{dS_q}{(\nabla E)_{k'}} M^2(\boldsymbol{q},\boldsymbol{k})\,\Phi_1\left(\frac{E}{T},\frac{\epsilon}{T}\right) \tag{6}$$

where dS_q is an element of area of the surface $F(\boldsymbol{q}+\boldsymbol{k}) = 0$; and $\Phi_1 = \Phi_+ + \Phi_-$.

Let both distribution functions be initially in equilibrium: $\phi_\epsilon = \phi_\epsilon^{(0)} = (e^t - 1)^{-1}$, where $t = \epsilon/T$, and $f_E = f_E^{(0)} = (e^\alpha + 1)^{-1}$, where $\alpha = (E - E_f)/T$.

We then have

$$\Phi_1(\alpha,t) = \phi_\epsilon^{(0)}(1-f_{E+\epsilon}^{(0)}) + (\phi_\epsilon^{(0)}+1)(1-f_{E-\epsilon}^{(0)}) = \frac{e^\alpha(e^\alpha+1)(e^t+1)}{(e^t-1)(e^{\alpha-t}+1)(e^{\alpha+t}+1)}. \tag{7}$$

For an electron which is near the fermi level, within the region of thermal smearing ($|\alpha| \lesssim 1$), the equilibrium functions reduce $\Phi_1(\alpha,t)$ to zero for those phonons for which $t \gg 1$. In the first term in $\Phi_1(\alpha,t)$ this takes place because the function $\phi_\epsilon^{(0)}$ is small for phonons with energies greater than T and hence the probability of absorbing these phonons is also small. In the second term the factor $(1-f_{E-\epsilon}^{(0)})$ reduces to zero because states with energy $E-\epsilon$ are occupied and the electron cannot therefore emit a phonon with $\epsilon \gg T$.

2.2. *Electrons with energy* $E = E_f$

It is clear from (6) and (7) that the scattering probability ν is a function of the energy α of the initial electron state. To make clear the dependence of ν on temperature and the shape of the fermi surface, we at first suppose that the electron energy is exactly equal to the fermi energy: $\alpha = 0$, so that (7) now becomes

$$\Phi_1(0,t) = 2e^t(e^{2t}-1)^{-1}. \tag{8}$$

After expressing $M^2(\boldsymbol{k},\boldsymbol{q})$ using (5), we examine three particular cases.

2.2.1. A cubic dependence of $\nu(T)$. Let the wave vector of a thermal phonon be

$$q_T \sim T/\hbar s \ll k_f \tag{9}$$

(both here and below k_f describes a characteristic dimension of the fermi surface, which differs for each specific case; in (9) k_f is the radius of curvature of the fermi surface at the point $\boldsymbol{k}$). If we now introduce a characteristic temperature $Q = k_f\hbar s$, the inequality in (9) can be written as $T \ll Q$. In general there is some temperature T for each k_f, below which the inequality in (9) is satisfied. However, in the temperature range 1–10 K which is most commonly used experimentally, the condition in (9) is satisfied for $k_f \approx K$ and $Q \approx \hbar s K = T_D$ (the Debye temperature). We shall therefore refer to (9) as describing a 'large' fermi surface.

By making a series expansion of the surface $F(\boldsymbol{k}) = 0$ around the point $\boldsymbol{k}$ and neglecting quadratic terms, we find that the region of integration in (6) is a plane in $\boldsymbol{q}$ space passing through the origin, with a normal parallel to the gradient of the fermi surface at the point $\boldsymbol{k}$, $\mathrm{d}S_q = 2\pi q\,\mathrm{d}q$ and

$$\nu = \frac{\Delta^2 T^3}{2\pi\hbar^4 \mu s^4 v}\int_0^\infty \frac{t^2 \mathrm{e}^t\,\mathrm{d}t}{\mathrm{e}^{2t}-1} = \frac{7\zeta(3)}{8\pi}\frac{\Delta^2 T^3}{\hbar^4 \mu s^4 v}; \qquad \zeta(3) = 1{\cdot}2. \tag{10}$$

It may happen that there is another sheet of the fermi surface near the point $\boldsymbol{k}$, at a distance $q_\mathrm{u} \ll q_\mathrm{T}$ (see, for example, figure 2, where this sheet is a consequence of Umklapp processes; it can also be just another part of a multiply-connected fermi surface). If (9) is also valid for the second part of the surface, we need to add a second similar expression to (10)

$$\nu_\mathrm{add} = \frac{\Delta^2 T^3}{2\pi\hbar^4 \mu s^4 v_1}\int_{t_\mathrm{u}}^\infty \frac{t^2 \mathrm{e}^t\,\mathrm{d}t}{\mathrm{e}^{2t}-1}, \qquad t_\mathrm{u} = \hbar s q_\mathrm{u}/T \tag{11}$$

(the subscript 1 on v means that the velocity refers to the second sheet of the fermi surface).

We emphasize once again that the simplified form of the matrix element in (5) can affect only the numerical coefficients in (10) and (11), not the form of the power law dependence of $\nu(T)$. This observation also applies to all the calculations described below.

2.2.2. Linear dependence $\nu(T)$. The opposite limiting case

$$q_\mathrm{T} \gg k_\mathrm{f}; \qquad Q \ll T \tag{12}$$

(here k_f is the maximum possible distance from the point $\boldsymbol{k}$ to another point on the fermi surface) is appropriate at high temperatures, or at helium temperatures for a small enough fermi surface $k_\mathrm{f} \lesssim (0{\cdot}05\text{–}0{\cdot}1)$ K. For all phonons which satisfy (1) and (2) we have $t \ll 1$, so that $\Phi_1(0, t) = t^{-1}$ and

$$\nu(T) = \frac{\Delta^2 T}{8\pi^2\hbar\mu s^2}\oint \frac{\mathrm{d}S_q}{(\nabla E)_{k'}} = \frac{\pi\Delta^2 T n_\mathrm{f}}{2\hbar\mu s^2} \tag{13}$$

($n_\mathrm{f} = (2/(2\pi)^3)\oint(\mathrm{d}S/\nabla E)$ is the density of states at $E = E_\mathrm{f}$).

2.2.3. Quadratic dependence of $\nu(T)$. When the electron dispersion law is highly anisotropic there is another possibility, which is realized in a number of cases. Suppose that we have a fermi surface in the form of a long cylinder and we consider a temperature range for which q_T is much greater than the cylinder radius but much less than its length:

$$k_{1\mathrm{f}} \ll q_\mathrm{T} \ll k_{2\mathrm{f}}. \tag{14}$$

The two-dimensional integral in (6) then becomes the product of two integrals, along the perimeter of the cylinder and parallel to its axis, and only one of these depends on T (Gantmakher and Dolgopolov 1971); so that

$$\nu(T) = \frac{\Delta^2}{2\pi^2\mu s}\oint \frac{\mathrm{d}q_\perp}{(\nabla E)_{k'}}\left(\frac{T}{\hbar s}\right)^2 \int_0^\infty \frac{t\,\mathrm{e}^t\,\mathrm{d}t}{\mathrm{e}^{2t}-1} = \frac{\pi}{8}\frac{m_\mathrm{c}\Delta^2 T^2}{\hbar^4 \mu s^3} \tag{15}$$

where $m_\mathrm{c} = (\hbar^2/2\pi)\oint(\mathrm{d}k/\nabla E)$ is the cyclotron mass of a section perpendicular to the cylinder axis. For a circular cylinder of radius $k_{1\mathrm{f}}$ the mass $m_\mathrm{c} = \hbar k_{1\mathrm{f}}/v$.

Thus the scattering probability can be proportional to the first power of T, or to T^2 or T^3, depending on the relative values of q_T and the fermi surface dimensions. The experimental observations of these dependences are discussed in § 6.

2.3. Hot electrons

We now consider a 'hot' electron above the fermi surface and outside the region of thermal smearing ($\alpha \gg 1$), for unperturbed electron and phonon distribution functions, $f_E = f_E^{(0)}$ and $\phi_\epsilon = \phi_\epsilon^{(0)}$. For such an electron the choice of phonons which can be emitted is much wider. To take a specific case, let us suppose that the heating is comparatively small, so that $\alpha \ll E_f/T$ and the difference between the fermi surface and the constant energy surface on which the electron lies is negligible. Naturally, as before, the scattering can be considered as elastic. The equation $F(\boldsymbol{q}+\boldsymbol{k}) = 0$, which determines the region of integration over $\boldsymbol{q}$ in (6), then remains the same as before.

The function $\Phi_1(\alpha, t)$ within the integral is now nonzero for phonons with energies t up to α, and over most of this range, specifically for $1 < t < \alpha$, $\Phi_1(\alpha, t) \approx 1$.

In (9), (12) and (14), which define the 'geometrically' various limiting cases, we now need to replace q_T by $q_\alpha = (E-E_f)/\hbar s \gg q_T$. The integrations lead to the following expressions:

$$q_\alpha \ll k_f: \quad \nu = \frac{\Delta^2}{12\pi\hbar^4 \mu s^4 v}(E-E_f)^3 \quad \text{(instead of (10))} \tag{16}$$

$$q_\alpha \gg k_f \gg q_T: \quad \nu = \frac{\Delta^2}{8\pi^2 \hbar \mu s} \oint_{F=0} \frac{dS_q\, q}{v_{k'}} \quad \text{(instead of (13))} \tag{17}$$

$$k_{1f} \ll q_\alpha \ll k_{2f}: \quad \nu = \frac{m_c \Delta^2}{4\pi\hbar\mu s^3}(E-E_f)^2 \quad \text{(instead of (15))}. \tag{18}$$

When q_α is less than any of the fermi surface dimensions (the cases described by (16) and (18)), the emission of a single phonon will return the electron practically to the fermi level. If $q_\alpha \gg k_f$, then at least q_α/k_f phonons must be emitted to dissipate the excess electron energy.

For a discussion of the scattering probability for electrons with intermediate values of α see below (figure 8).

2.4. Electrons in a high magnetic field

All the discussion so far has assumed that the magnetic field H was zero. However, a sufficiently high magnetic field can change the probability of electron–phonon scattering, at any rate for parts of the fermi surface which lie close to extremal sections (Gantmakher 1972).

In a magnetic field the electron energy spectrum undergoes the usual Landau quantization and takes the form (for $\boldsymbol{H} \parallel z$)

$$E = n\hbar\Omega + \hbar^2 k_z^2/2m^* \tag{19}$$

where n is an integer; $\Omega = eH/m_c c$ is the cyclotron frequency, m_c is the cyclotron mass, and m^* is the effective mass for motion along the magnetic field. As is well known, the cyclotron mass is given by the integral

$$m_c = \frac{\hbar}{2\pi} \oint \frac{dk}{v_\perp} \tag{20}$$

over a contour given by the intersection with the fermi surface of a plane perpendicular to $\boldsymbol{H}$; $v_\perp$ is the component of the electron velocity in this plane.

The quantum numbers for an electron in a magnetic field are n, k_x and k_z (the quantity ck_x/eH determines the orbit centre, and the energy is independent of k_x, so the spectrum is degenerate). However, when n is large and the quasiclassical approximation is valid, we can use the usual classification of states in terms of the three components of the wave vector. For a high enough field ($\Omega/\nu \gg 1$) the allowed states of the electronic spectrum in k space become a series of nested cylinders with cross sectional area $S_n = 2\pi neH/\hbar c$. The shape of these cylinders depends on that of the fermi surface; for an isotropic quadratic spectrum the cylinders are circular.

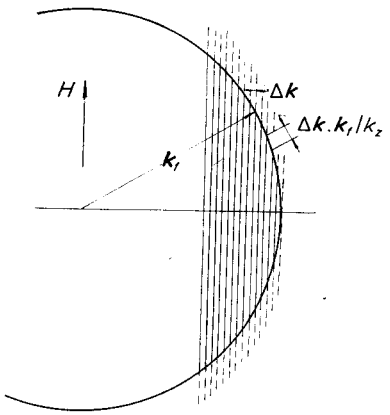

Figure 3. Spectrum of electrons in a magnetic field—a system of nested cylinders. The fermi sphere divides occupied from empty states on the cylinders.

The use of k_x, k_y and k_z as quantum numbers allows us to apply the law of conservation of quasimomentum (equation (2)) in the calculation of the scattering probability. The correctness of this approach for $n \gg 1$, $qv/\Omega \gg 1$ is confirmed by a rigorous calculation.

For simplicity let us consider an isotropic quadratic spectrum such that $E_f \gg T \gg m^* s^2$. The occupied states on the cylinders lie within a sphere of radius k_f (see figure 4). In the neighbourhood of the extremal section the separation of the cylinders is $\Delta k = eH/\hbar k_f c$. We consider an electron with energy $E \approx E_f$ and wave vector $\boldsymbol{k}(|k| \approx k_f)$, located on a cylinder with sufficiently large n. If, in the neighbourhood of $\boldsymbol{k}$, the separation between the intersections of successive cylinders with the fermi sphere $\Delta k k_f/k_z = eH/\hbar k_z c \ll q_T$, scattering by phonons can produce transitions with $\Delta n \gg 1$ and the scattering probability ν is the same as for $H = 0$ (see equation (10)).

It is, however, not difficult to see that there can occur, at sufficiently high fields and near the extremal section where k_z is small, a region for which the opposite inequality is valid

$$\frac{eH}{\hbar k_z c} \gg q_T, \qquad \frac{\hbar\Omega}{T}\frac{s}{v}\frac{m_c}{m^*} \gg \frac{k_z}{k_f}. \tag{21}$$

In this region of wave vector space the probability of transitions with $\Delta n \neq 0$ is exponentially small, so all transitions due to phonon scattering take place with $\Delta n = 0$.

We can easily derive the lower boundary on the magnetic field for which this region exists. The fermi cut-off is smeared in energy by T and therefore, for $n\hbar\Omega = E_f$, the nth cylinder touches the fermi sphere of radius k_f and contains electrons only with

$$k_z \lesssim \hbar^{-1}(2m^* T)^{1/2}. \tag{22}$$

By demanding that these electrons satisfy (21), we find

$$\hbar\Omega \gtrsim T\left(\frac{T}{m_c s^2}\right)^{1/2}\left(\frac{m^*}{m_c}\right)^{1/2}. \tag{23}$$

The collision frequency for transitions with $\Delta n = 0$ is

$$\nu(k_z) = \frac{\Delta^2}{4\pi\hbar\mu s} g \int q\, \mathrm{d}^2 q \sum_{\pm} \Phi_{\pm}(\alpha, t)\, \delta(E_{k'} - E_k \mp \epsilon) \tag{24}$$

where, as distinct from (4) and (6), the integration is over a surface and not a volume, and there is an additional factor $g = \Omega/2\pi v_\perp$ which is the degeneracy of the states on the cylinder. If the cylinder has a circular cross section with radius k_f, then $g = (2\pi\hbar)^{-1} eH/k_f c$.

The factor g affects the magnetic field dependence of ν; at the same time the power of T in the function $\nu(T)$ is reduced, because after the elimination of the δ-function in (24) the integration is along a line on the cylinder, not over a surface.

The argument of the δ-function in (24) is given by

$$\pm\frac{\hbar^2 k_z q_z}{m^*} + \frac{\hbar^2 q_z^2}{2m^*} \mp \hbar q s.$$

It is clear from this expression that the region described by (21) can be divided into two sub-regions. In the immediate neighbourhood of the central section $k_z = 0$, where for the majority of transitions $k_z \ll q_z$, the frequency of collisions with phonons is

$$\begin{aligned}\nu(k_z) &= \frac{\Delta^2\,\Omega}{8\pi^2\hbar\mu s v}\int\int q\,\mathrm{d}q_x\,\mathrm{d}q_z\,\Phi_+(\alpha,t)\,\delta\left(\frac{\hbar^2 q_z^2}{2m^*} - \hbar q s\right)\\ &= \frac{1{\cdot}5}{2\sqrt{2}\pi^2}\frac{\Delta^2}{\hbar^4\mu s^4 v}(\hbar\Omega)(m^* s^2)^{1/2} T^{3/2}\end{aligned} \tag{25}$$

(here $q = (q_x^2 + q_z^2)^{1/2}$; and the factor 1·5 is the numerical value of the integral $\int_0^\infty e^t(e^{2t}-1)^{-1} t^{1/2}\,\mathrm{d}t$). The upper limit on k_z for this region is defined by the condition $k_z \ll q_T(2mT)^{1/2}/\hbar$. For sufficiently high fields there is another intermediate region

$$\frac{(2mT)^{1/2}}{\hbar} \ll k_z \ll k_z\frac{\hbar\Omega}{T}\frac{s}{v}\frac{m_c}{m^*} \tag{26}$$

for which the argument of the δ-function is now $\hbar^2 k_z q_z/m^* - \hbar q s$, so that instead of (25) we find

$$\nu(k_z) = \frac{1}{32}\frac{\Delta^2 m^*}{\hbar^5\mu s^3 v k_z}(\hbar\Omega)\,T^2. \tag{27}$$

It is curious to observe that the scattering described by (25) and (27) cannot be regarded as elastic, because the phonon energy $\hbar q s$ cannot be neglected in the argument of the δ-function.

3. Electrical resistivity

So far we have discussed the scattering probability $\nu(\boldsymbol{k})$, or the collision frequency, which comes to the same thing, of a single electron. The inverse quantity $\tau(\boldsymbol{k}) = \nu^{-1}(\boldsymbol{k})$ is the mean lifetime of an electron in a state between two collisions with phonons. It is natural to ask what is the relation between this time τ, which has a clearly defined physical significance, and the electron–phonon relaxation times τ_i which are measured experimentally in various situations.

We begin with measurements of the DC electrical resistance. The interpretation of these is discussed in a large number of papers and reviews (for example MacDonald 1956, Gurzhi 1968, Springford 1971) and here we limit ourselves to a discussion of the basic factors which determine the salient features of the physical behaviour.

3.1. Small-angle scattering

If a single scattering process transfers an electron to a state with any direction of $\boldsymbol{v}_k$, with practically equal probability, this is referred to as isotropic scattering. Impurity scattering in a metal, for example, is isotropic because the impurity potential is always short range as a result of the strong screening.

Phonon scattering is by no means always isotropic. It is isotropic at high temperatures when the inequality in (12) is valid, as can be seen from the expression under the integral in (13). It is also isotropic when the inequality in (14) is valid, since transitions to all points along the perimeter of the cylinder are in practice equally probable, and the velocity $\boldsymbol{v}_{k'}$ can take any direction in the plane perpendicular to the axis of the cylindrical fermi surface. However, phonon scattering becomes strongly anisotropic when the inequality in (9) is valid, because then most scattering processes change the direction of the velocity by an angle

$$\theta = q_T/k_f \approx T/Q \ll 1.$$

(If $k_f \approx K$, then $\theta \approx T/T_D$.)

The current through the sample is determined by the non-equilibrium perturbation Δf to the distribution function:

$$j = \frac{2e}{(2\pi)^3}\int \mathrm{d}^3k\,\Delta f v. \tag{28}$$

When one of the electrons which contributes to the integration in (28) makes a transition from state $\boldsymbol{k}$ to state $\boldsymbol{k}'$ as a result of a collision, its contribution to the current changes by $e\Delta\boldsymbol{v} = e(\boldsymbol{v}_{k'} - \boldsymbol{v}_k)$. This change is a measure of the effectiveness of the collision, and it must enter into the expression for the relaxation time for electrical conductivity—the so-called transport relaxation time—together with the collision probability. The well-known expression for the transport relaxation time under conditions of elastic scattering is

$$\tau_{tr}^{-1} = \int (1-\cos\theta)\,\nu_q(\theta)\,\mathrm{d}\mathcal{O} \tag{29}$$

(θ is the scattering angle and $\mathrm{d}\mathcal{O}$ is the element of solid angle), which compared with (4) contains an additional weighting factor $(1-\cos\theta)$ (see, for example, Peierls 1955 or Ziman 1960). For small θ this factor is $\frac{1}{2}\theta^2 \approx \frac{1}{2}(q/k_f)^2$.

We can use (29) to calculate the conductivity only after a whole series of simplifying assumptions: that the constant energy surfaces are spherical (so that θ is both the angle between $\boldsymbol{k}$ and $\boldsymbol{k}'$ and the angle between $\boldsymbol{v}_k$ and $\boldsymbol{v}_{k'}$), that ν_q depends only on θ and is independent of $\boldsymbol{k}$, etc. However, the fact that the effectiveness of small-angle scattering is proportional to the square of the angle is of much more general importance, since the effectiveness is essentially determined by comparing the old velocity with the projection on it of the new velocity.

Thus phonon scattering is anisotropic under the conditions in (9); the conductivity is determined by the transport relaxation time not the total relaxation time, and the effectiveness of collisions is temperature dependent. This is why the resistivity ρ varies with temperature as T^5 (the Bloch–Grüneisen law), ie more rapidly than the total collision frequency in (10).

3.2. Diffusion approximation

The fact that the wave vector q_T of a thermal phonon is small compared to k_f, together with the condition $\boldsymbol{q} \perp \nabla E$, enables us to discuss the change in electron wave vector in successive collisions of phonons in terms of the diffusion of the electron over the fermi surface (Klemens and Jackson 1964). If in real space the particle moves with constant velocity between collisions and then suddenly changes its velocity in the collision, the point on the fermi surface which represents the electron does not move between collisions (or in the presence of a constant magnetic field it rotates along a cyclotron orbit) and in a collision it is suddenly displaced in the surface by a distance $\boldsymbol{q}$. Since the average value of the wave vector of phonons interacting with electrons is $|\boldsymbol{q}| \approx q_T$, and the direction of the vectors $\boldsymbol{q}$ is arbitrary in the tangent plane, the electron will be displaced from its initial point by a distance $q_T\sqrt{P}$ after a large number P of collisions.

The well-known Bloch–Grüneisen law for the temperature dependence of the resistance for $T \ll T_D$ follows immediately from this. To be effectively scattered the electron must diffuse some fixed temperature independent distance κ on the fermi surface, and this requires $P \approx (\kappa/q_T)^2$ collisions. These collisions occupy a time

$$\tau_{tr} = \frac{P}{\nu} = \frac{\kappa^2}{q_T{}^2 \nu} \tag{30}$$

where the collision frequency ν is given by (10). Since $\nu \propto T^3$, it follows that $\tau_{tr} \propto T^5$, and the resistivity $\rho = m^*/Ne^2\tau_{tr} \sim T^5$ (N is the electron density).

It is sometimes convenient to introduce a diffusion coefficient $\mathscr{D}$, equal to the mean square displacement in unit time of the electron along some particular direction:

$$\mathscr{D} \approx q_T{}^2 \nu \sim T^5; \qquad \tau_{tr} = \kappa^2/\mathscr{D} \tag{31}$$

and to discuss the whole problem in 'diffusion language' which is mathematically equivalent to the kinetic equation. The most logical and elegant approach of this kind is due to Pippard (1964, 1968). The application of an electric field $\mathscr{E}$ displaces the fermi surface as a whole in $\boldsymbol{k}$ space, with velocity $e\mathscr{E}/\hbar$. This also continuously generates a perturbation to the distribution function at each point in $\boldsymbol{k}$ space at a rate

$$\left(\frac{\partial \Delta f}{\partial t}\right)_{gen} = -\left(\frac{\partial f^{(0)}}{\partial E}\right) e\mathscr{E}.\boldsymbol{v}. \tag{32}$$

Since $\partial f^{(0)}/\partial E \approx -\delta(E - E_f)$, this generation takes place only at the fermi surface.

This process can be considered as the creation of new electrons at those parts of the surface where $\mathscr{E}.\boldsymbol{v}>0$, and of new holes where $\mathscr{E}.\boldsymbol{v}<0$; these new particles diffuse over the surface and annihilate each other whenever they meet. The search for a stationary value of Δf thus reduces to the solution of a diffusion equation. The distribution of sources over the fermi surface is given by (32), and the diffusion coefficient by (31); the specific features of a particular problem are reflected in the distribution of particle sinks, the regions of most intense annihilation, ie in the formulation of the boundary conditions for the diffusion equation.

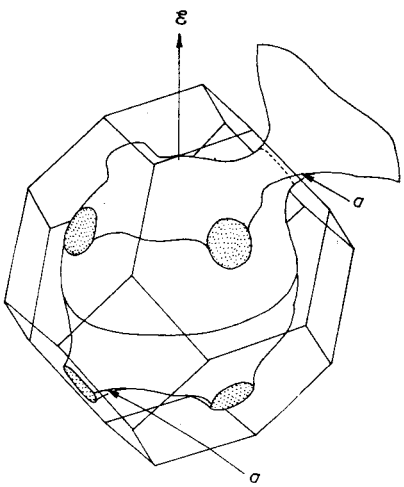

Figure 4. Fermi surface of copper. The lines of the intersection of the fermi surface with the Brillouin zone boundaries are additional sinks. Two equivalent points on the fermi surface are shown by the letter *a* (from Pippard 1964).

In the kinetic equation the change in the distribution function due to collisions includes both the scattering of particles out of a given state and scattering into this state from other states. (The quantity $\nu(\boldsymbol{k})$ discussed in the previous section is the probability of scattering out of a given state.) The diffusion equation automatically takes account of both these processes, since a particle created at the point $\boldsymbol{k}$ can diffuse to a region of the fermi surface which is farther from the sinks than the point $\boldsymbol{k}$. On the other hand, the continuity of the density of diffusing particles ensures that the appearance of new sinks reduces the density Δf over the whole surface.

3.2.1. Examples. We illustrate the above remarks with examples taken from the work of Pippard (1964). If the fermi surface is spherical it is clear that the sinks are situated on the great circle (the equator) perpendicular to $\mathscr{E}$, where $\Delta f = 0$. When it reaches the equator, an electron annihilates with a hole that has diffused to the equator from the other hemisphere. Let us now consider the fermi surface of copper, which consists of a system of spheres periodically repeated in $\boldsymbol{k}$ space and connected to each other by small necks. One of these spheres is shown in figure 4. This surface has additional sinks at the necks, because in this region, where the radius of curvature of the surface is relatively small, a small change in the wave vector can produce a large change in the direction of the velocity, and an electron

which has diffused a small distance across the neck will find itself almost immediately in the other hemisphere. The presence of extra sinks must, of course, affect the value of τ_{tr} (see equation (31)), and τ_{tr} will depend on the position of the equator with respect to the necks ie on the direction of the electric field $\mathscr{E}$. The effectiveness of scattering becomes anisotropic, not because of the phonon spectrum or the deformation potential, but because of the shape of the fermi surface itself.

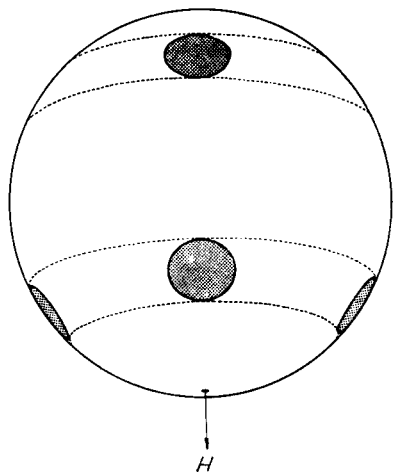

Figure 5. Schematic representation of the fermi surface of copper. The broken lines show sinks in a high magnetic field (from Pippard 1964).

Copper in a magnetic field provides another interesting example. Suppose that we are interested in longitudinal magnetoresistance in a field $\boldsymbol{H} \| \mathscr{E} \| [001]$, and H is large enough that the cyclotron frequency $\Omega \gg \nu$. Then the sinks, together with the equator, are given by the broken lines in figure 5 instead of the perimeters of the necks. In fact the contribution to the current, as given by (32), of an electron created at some point on the surface is given by the orbital average of its velocity parallel to the field

$$\bar{v}_{\mathscr{E}} = \frac{\hbar}{2\pi m_c} \oint \frac{v_{\mathscr{E}} \, dk}{v_\perp}.$$

Scattering along the orbit is therefore unimportant from the point of view of longitudinal magnetoresistance; the relevant diffusion becomes one-dimensional, transverse to the cyclotron orbits. The broken lines in figure 5 distinguish those orbits which have an opposite sense of traversal, as a result of the multiple connectivity of the surface. Transitions across these lines change $\bar{v}_{\mathscr{E}}$ discontinuously by a large amount.

3.3. Umklapp processes

The correctness of the above discussion rests on the assumption that the phonon distribution function is in equilibrium, $\phi_\varepsilon = \phi_\varepsilon^{(0)}$, which means that there must be some mechanism for dissipating momentum. If there is not, the phonons are dragged along by the electrons, the difference between ϕ_ε and $\phi_\varepsilon^{(0)}$ becomes appreciable, and the variation $\rho \propto T^5$ is replaced by an exponential drop in electrical resistivity as the temperature is reduced (eg see Peierls 1955).

Umklapp processes guarantee a mechanism for the dissipation of momentum. It therefore often follows just from the topology of the fermi surface that phonon drag will not occur. For example, for an open fermi surface there are always regions near the zone boundary for which collisions with $\boldsymbol{K} \neq 0$ will take place right down to $T = 0$, no matter how the unit cell of the reciprocal lattice is chosen. If the fermi surface is closed but its separate pieces come close to each other, Umklapp processes will occur for $q_T \geqslant q_u$ (see figure 2), and the corresponding temperature can be quite low. Phonon drag also does not occur when the number of electrons in the metal is equal to the number of holes, because electrons and holes acquire opposite extra momenta from the electric field.

The practical outcome of these considerations is that the only materials in which the exponential drop in ρ with decreasing temperature can be observed are the alkali metals, but even in these it has not yet been observed (Ekin and Maxfield 1971). We shall return to this problem later, after discussing a second aspect of the influence of Umklapp processes on the electrical resistivity. At this point we just note that the diffusion equation can be derived from the kinetic equation even if phonon drag by electrons is taken into account (Gurzhi and Kopeliovich 1971); the problem is similar to that of diffusion in a flowing liquid, but the flow velocity of the 'phonon liquid' is in its turn determined by the rate of creation of the diffusing particles.

3.4. Hot spots

The above discussion of the anisotropy of phonon scattering has been in terms of the dependence of the scattering probability on the final state $\boldsymbol{k}'$ of the electron, for a given initial state $\boldsymbol{k}$. It is also clear that another kind of anisotropy can be associated with electron–phonon scattering. This is again due to a specific feature of the electron spectrum—the strong dependence of τ_{tr} on $\boldsymbol{k}$.

First, the fermi surface of most metals contains both regions with large radii of curvature k_f, where (10) and (30) are valid, and other regions with small radii of curvature, where $\tau_{tr} \approx \nu^{-1}(\boldsymbol{k})$ and $\nu(\boldsymbol{k})$ is given by equations like (13) or (15). One would think that the small regions give only a small contribution to the resistivity, but this is not always the case. It was shown by Gurzhi and Kopeliovich (1971), using a model fermi surface consisting of 'large' surfaces joined by narrow necks and including phonon drag effects, that the temperature dependent part of the electrical resistivity is determined by just these necks, in fact by the resistance which they present to diffusive particle fluxes on the fermi surface. For a given ratio of the parameters in this model, the electrical resistivity can be proportional to T^4, not to T^5 as is usual.

Secondly, τ_{tr} is strongly affected by situations in which the fermi surface consists of several sheets, in particular by the presence of regions with large radii of curvature k_f which are comparatively close to each other in $\boldsymbol{k}$ space. These regions can occur because of a 'trivial' multiple connectivity of the fermi surface (eg as in tin) and as a result of Umklapp processes (see figure 2). It is clear from (10) and (11) that the effect of multiple sheets on the value of ν is less marked, increasing it roughly speaking by a factor of two. However, whilst scattering within a single sheet produces only a small change in electron velocity, as in (9), and the effectiveness of this scattering contains a factor of order $(T/Q)^2$, scattering to another sheet must almost always be accompanied by a large change in velocity (either in

magnitude or, as in Umklapp processes, in direction). Therefore, as distinct from the function $\nu(\boldsymbol{k})$, the local values of $\tau_{tr}(\boldsymbol{k})$ change by a factor of $(Q/T)^2$ in these regions ie by two to four orders of magnitude (these regions have been named 'hot spots' by Young 1968).

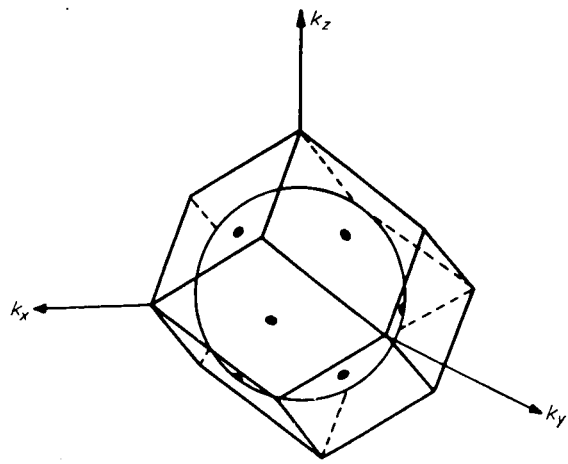

Figure 6. 'Hot spots' on the fermi surface of potassium, which has a BCC lattice, lie in the ⟨110⟩ directions. Cf figure 5: on the fermi surface of copper the 'hot spots' have become necks in the [111] directions (from Young 1968).

The distribution of hot spots on the fermi surface of an alkali metal is shown in figure 6. It has repeatedly been shown experimentally that the resistivity of potassium decreases more quickly than T^5 at helium temperatures. Phonon-drag effects and the freezing out of the extra scattering channel through the hot spots will both lead to this more rapid decrease in the temperature dependent part of the electrical resistivity. However, it is doubtful whether it is possible to separate these two effects. It is true that Ekin and Maxfield (1971) obtained good agreement between their experimental data and calculated curves which were obtained by neglecting phonon drag effects and including only the freezing out of the scattering channels through hot spots. On the other hand, when Umklapp processes have been frozen out for the fermi surface of an alkali metal, and $\rho > \rho_0$, there is no mechanism for preventing phonon drag. It is possible that the effect of phonon drag is numerically much smaller than that of the freezing out, but this question has not yet been investigated.

The presence of hot spots leads to a series of non-trivial effects even for a spherical fermi surface. It was shown by Kagan and Zhernov (1971) that the perturbation to the distribution function Δf contains, as well as a term of the same symmetry as the field term (equation (32)) in the kinetic equation, other terms which reflect the symmetry of the distribution of hot spots on the fermi surface, and over a given temperature region these can reduce the resistivity by a factor of three or so. The presence of isotropic impurity scattering smooths this effect, because large-angle scattering by phonons at the hot spots has an equivalent effect to isotropic scattering at impurities. At helium temperatures and for the values of q_u found in real metals these two scattering mechanisms are of comparable strength for impurity concentrations of 10^{-3} to 10^{-5}. This can give rise to considerable deviations from Matthiessen's rule at very low impurity concentrations. These deviations have

been repeatedly observed experimentally (eg by Tsoi 1969 and by Caplin and Rizzuto 1971).

The application of a magnetic field makes the function Δf isotropic, or at least partially so, because of the motion of electrons around the cyclotron orbits which pass through the hot spots. This effect was considered by Young (1968) and it was shown that in principle it was possible to use this effect to explain the linear field variation of the transverse magnetoresistance which is observed in alkali metals.

4. Kinetic effects from extremal trajectories

The electrical resistivity, together with a number of other 'traditional' properties of metals, such as the Hall effect, thermal conductivity and specific heat, are all integral parameters of the metal in that they are determined by electrons over the whole fermi surface. We now turn to experiments of a different type, where the effects are due to the parameters of particular groups of electrons on the fermi surface. In this section we discuss the possibility of measuring the frequency of electron–phonon collisions by using RF size effects, cyclotron resonance, ultrasonic absorption and resonance effects due to magnetic surface levels.

4.1. General principles

Theories of all the effects listed above and also of other similar effects are based on the relaxation time approximation. The value of ν_{eff} which appears in the kinetic equation in these theories is an independent parameter. We have already seen in the previous section that ν_{eff} can bear a very complicated relation to the total collision frequency, and in all cases the clarification of this relation necessitates additional analysis, based on the existing theory.

4.1.1. Nonequilibrium perturbations of the distribution function. All the effects under discussion have one feature in common: they are determined by a perturbation to the distribution function Δf which is nonzero only over a small region Σ of the fermi surface. Although the position on the fermi surface of this region Σ can vary from point to point in the crystal, at any particular point in real space it can be roughly represented by a rectangle with two characteristic dimensions $\Delta_1 k, \Delta_2 k \ll k_{\text{f}}$. We shall leave estimates of these parameters in particular cases until later; at this point we merely note that at helium temperatures $\Delta_1 k$ and $\Delta_2 k$ can be either greater than or less than q_{T}, the momentum of a thermal phonon. The most interesting case is

$$q_{\text{T}} \gg \min(\Delta_1 k, \Delta_2 k). \tag{33}$$

Since collision with a phonon shifts the electron by a distance q_{T} on the fermi surface, it follows from (33) that any collision will take the electron outside the region Σ (see figure 7). To determine the amplitude of the effects considered it is not important to know how far from the initial point $\boldsymbol{k}$ the electron finds itself after scattering, the important feature is that it has been scattered outside the effective region Σ. It therefore follows that when the condition in (33) is satisfied the phonon part ν_{ph} of the effective collision frequency ν_{eff} in the kinetic equation is

$$\nu_{\text{ph}} = \nu_{\text{eff}} - \nu_0 \tag{34}$$

(ν_0 is the frequency of collisions with static defects) and is determined by the total relaxation time (equation (4)) and not by the transport relaxation time (equation (29)) (Azbel' and Kaner 1958).

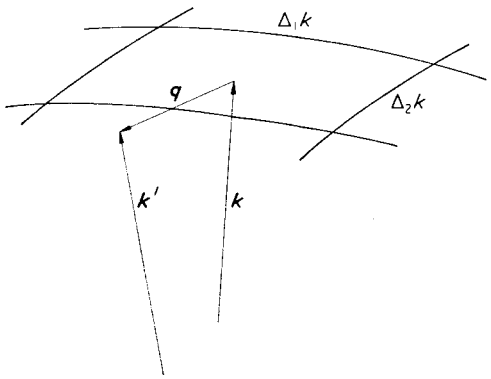

Figure 7. Scattering process which removes an electron from the effective zone Σ on the fermi surface.

This function $\nu_{\rm ph}$ differs somewhat from the functions in (10), (13) and (15) for two reasons. First, the amplitude of the effects considered is determined, strictly speaking, by the rate of change due to collisions of the increment Δf which had already been produced in the region Σ by some other means. This change is produced as a result of both scattering out of the state $\boldsymbol{k}$:

$$\Delta N_{\rm lose} \sim \Delta f[\phi_\epsilon(1-f_{E+\epsilon})+(\phi_\epsilon+1)(1-f_{E-\epsilon})] \tag{35}$$

and of scattering into the state $\boldsymbol{k}$ from other states, according to the Pauli principle:

$$\Delta N_{\rm gain} \sim -\Delta f[\phi_\epsilon f_{E-\epsilon}+(\phi_\epsilon+1)f_{E+\epsilon}]. \tag{36}$$

The total change in the number of particles, normalized to one electron, is given by (Sharvin and Bogatina 1969)

$$-\frac{\Delta N}{\Delta f}=\frac{1}{\Delta f}(\Delta N_{\rm lose}-\Delta N_{\rm gain})\sim 2\phi_\epsilon+1+f_{E+\epsilon}-f_{E-\epsilon}$$

$$=\frac{(e^\alpha+1)^2(e^t+1)}{(e^t-1)(e^{\alpha-t}+1)(e^{\alpha+t}+1)}\equiv\Phi_2(\alpha,t). \tag{37}$$

As in (7), we use here the equilibrium distribution functions, because $\Delta f = 0$ over most of the fermi surface.

The difference between the functions $\Phi_2(\alpha, t)$ and $\Phi_1(\alpha, t)$, which were introduced in (7), is illustrated graphically in figure 8. For negative α the integral

$$\mathscr{T}_1(\alpha)=\int_0^\infty t^2\Phi_1(\alpha,t)\,dt$$

which contributes to $\nu(T)$ (see equations (6) and (10)) tends to zero, because the larger the value of $|\alpha|$, the smaller is the number of unoccupied states around the electron into which it can be scattered by thermal phonons. However, the perturbation to the distribution function in the region $\alpha<0$ consists of additional unoccupied states, 'holes' in the electron distribution. The lifetime of these holes (which should not be confused with holes in semiconductors!) decreases as $|\alpha|$

increases, because of the increased number of spontaneous transitions from the upper occupied electron levels with the emission of non-thermal phonons. It is natural to expect that the lifetimes of electrons and holes with the same value of $|\alpha|$ are the same: a perturbation of the distribution function for negative α is dissipated at the same rate as one for positive α. For $\alpha = 0$ the integral

$$\mathscr{T}_2(0) = \int_0^\infty t^2 \Phi_2(0, t)\, dt = 2\mathscr{T}_1(0)$$

4.1.2. Averaging over energy. A second distinction between the measured value of ν_{ph} and that which appeared in (10), (13) and (15) is related to the dependence $\nu(\alpha)$.

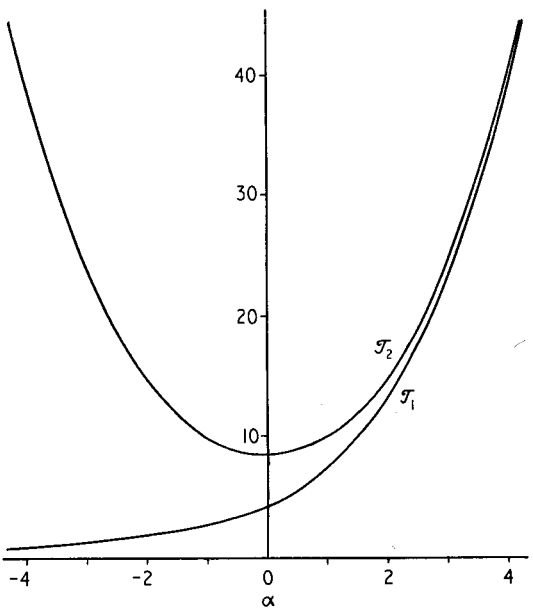

Figure 8. Graphs of the functions $\mathscr{T}_{1,2} = \int_0^\infty t^2 \Phi_{1,2}(\alpha t)\, dt$

In any practical experiment we are dealing with some range of initial electron energies, and it is necessary to average over these. The situation is complicated by the fact that usually the measured quantity A is not proportional to the collision frequency ν_{eff}, but has some more complicated dependence. For example, as we shall see below, in many cases $A \sim \exp(-\Gamma\nu_{eff})$, where Γ is some dimensioned coefficient.

When all the electrons of interest lie within the region of thermal smearing of the function $f_E^{(0)}$, ie, when $|\alpha| < 1$ for all the electrons which are relevant to the experiment, this difficulty can be avoided by using the fact that ν varies little compared to its average value over this range, so that in a linear approximation for the average values $\overline{A(\nu)} = A(\bar{\nu})$. To calculate $\bar{\nu}$ we use the fact that the perturbation Δf obtained by solution of the linearized Boltzmann equation is proportional to $(-\partial f^{(0)}/\partial E)$ and we can average (37) over the initial electron energies contributing to Δf before integrating over S_q in (6). Since the ratio between Δf and $\partial f^{(0)}/\partial E$ can be considered constant along the normal to the fermi surface in its immediate

neighbourhood, we can write

$$\bar{P}_2(t) = \frac{\int_0^\infty \Delta f \Phi_2(\alpha, t)\,\mathrm{d}E}{\int_0^\infty \Delta f\,\mathrm{d}E} = \int_{-\infty}^{\infty} \frac{\mathrm{e}^\alpha \Phi_2(\alpha, t)\,\mathrm{d}\alpha}{(\mathrm{e}^\alpha+1)^2} = \frac{2t\,\mathrm{e}^t}{(\mathrm{e}^t-1)^2}. \tag{38}$$

Replacing $\bar{P}_1(0,t)$ by $\bar{P}_2(t)$ in (10) and (15) changes only the definite integrals and consequently the numerical coefficient in (10) is increased by a factor of $\frac{24}{7}$, whilst that in (15) is increased by $\frac{8}{3}$. Since for $t \ll 1$ we have $\bar{\Phi}_2(t) \approx 2\Phi_1(0,t) \approx 2t$, the coefficient in (13) is doubled. As a result we obtain:

$$q_T \ll k_f: \quad \nu_{ph} = \frac{1}{2\pi} \frac{\Delta^2 T^3}{\hbar^4 \mu s^4 v} \int_0^\infty \frac{t^3 \mathrm{e}^t\,\mathrm{d}t}{(\mathrm{e}^t-1)^2} = \frac{3\zeta(3)}{\pi} \frac{\Delta^2 T^3}{\hbar^4 \mu s^4 v}; \qquad \zeta(3) = 1, 2, 0 \tag{39}$$

$$k_{1f} \ll q_T \ll k_{2f}: \quad \nu_{ph} = \frac{1}{\pi} \frac{m_c \Delta^2 T^2}{\hbar^4 \mu s^3} \int_0^\infty \frac{t^2 \mathrm{e}^t\,\mathrm{d}t}{(\mathrm{e}^t-1)^2} = \frac{\pi}{3} \frac{m_c \Delta^2 T^2}{\hbar^4 \mu s^3} \tag{40}$$

$$k_f \ll q_T: \quad \nu_{ph} = \pi \frac{\Delta^2 n_f T}{\hbar \mu s^2}. \tag{41}$$

The quantity ν_{ph} in (39)–(41) is in fact the collision frequency which is measured in the experiments discussed below, provided the condition in (33) is satisfied. The region of the fermi surface to which this value of ν_{ph} refers depends on the geometry in a particular experiment. Usually it is the result of averaging along an extremal orbit on the fermi surface.

4.1.3. The diffusion limit and an interpolation formula. If the opposite inequality to that in (33) is valid, we must return to the diffusion approach, but with a value of κ different from that for a DC current; the line of sinks can now be considered as being along the perimeter of the effective region. The parameter ν_{ph} in (34) is now replaced by another parameter ν_{ph}^*, which is no longer given by (39)–(41), but because of the different κ it is also different from ν_{tr} which determines the electrical resistivity. Equation (34) should itself be treated with caution, since we have seen that nonlinear interference effects are possible as a consequence of the diffusion origin of ν_{ph}^*.

These two cases ($q_T \ll \Delta_{1,2} k$ and $q_T \gg \Delta_{1,2} k$) can be distinguished directly from the experimental results, without any preliminary estimates: $(\nu_{eff} - \nu_0) \sim T^5$ for diffusive scattering, whilst the total collision frequency follows a power law dependence, with an exponent less than 3 (see equations (39), (40) and (41)).

The intermediate case $q_T \approx \Delta_1 k, \Delta_2 k$ may of course also occur. Experimental results may then be analysed by using an interpolation expression such as that proposed by Myers *et al* (1972):

$$\nu_{ph} = C_1 T^5 \int_0^{t_1} \frac{t^5 \mathrm{e}^t\,\mathrm{d}t}{(\mathrm{e}^t-1)^2} + C_2 T^3 \int_{t_1}^\infty \frac{t^3 \mathrm{e}^t\,\mathrm{d}t}{(\mathrm{e}^t-1)^2}. \tag{42}$$

Here $t_1 \approx \hbar \Delta_{1,2} ks/T$ is determined by some average value of $\min(\Delta_1 k, \Delta_2 k)$ over the orbit, and is in practice a fitting parameter like the constants C_1 and C_2. The expressions within the integrals in (42) are somewhat different to those in the paper referred to above, because they used a simplified form of the function $\Phi_2(\alpha, t)$. It has been shown that this approximation is justified in the calculation of the electrical resistivity (eg see Ziman (1964)).

4.2. *Radio-frequency size effects*

When the surface impedance of a plane-parallel metal plate is measured as a function of the magnetic field H, singularities occur in fields such that the plate thickness d is an integral multiple of a characteristic dimension of an extremal electron trajectory, and these are the lines of the radio-frequency size effect (RFSE)

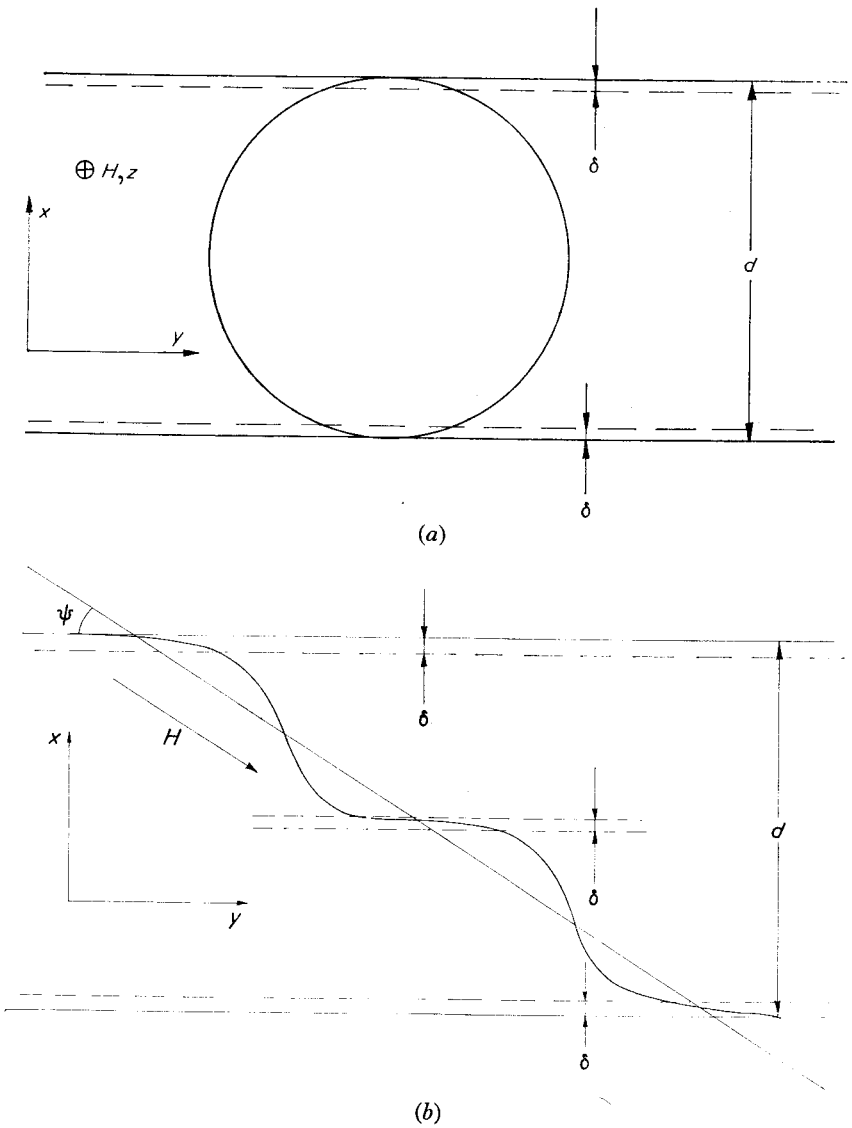

Figure 9. Shape of electron trajectories in RFSE: (*a*) for an extremal closed trajectory; (*b*) at a limiting point.

(Gantmakher 1967). The relative width of these lines is $\Delta H/H \sim \delta/d$, where δ is the skin depth. The experimental geometry for two types of RFSE is shown in figure 9; these are for closed trajectories and for limiting points, and these two examples will illustrate all aspects of the measurement of the mean free path l using the RFSE. The amplitude A of the RFSE line is governed by the probability that an electron will

traverse, without being scattered, a path λ along the trajectory from one side of the plate to the other. If the electron collides with the surface after arriving at the other side of the plate, as in the case of RFSE from a limiting point (figure 9(*b*)), then

$$A \sim \exp\left(-\frac{\lambda}{l}\right) = \exp\left(-\frac{2\pi n \nu_{\text{eff}}}{\Omega}\right) \tag{43}$$

where n is the number of turns along the cyclotron orbit made by the electron in the path λ; and ν_{eff} is the effective collision frequency at scattering centres of all types (Gantmakher and Sharvin 1965). For RFSE from a limiting point the lines occur at fields $H_n = nH_1$ corresponding to $n = 1, 2, 3, \ldots$. H_1 is determined by the plate thickness, the field tilt ψ, and the mean radius of curvature of the fermi surface at the limiting point: $H_1 = 2\pi_T k_f c\psi/ed$. The amplitude of the lines $A \sim \exp(-2\pi m_c c\nu_{\text{eff}}/eH_1)$, where the cyclotron mass m_c and the collision frequency ν_{eff} refer to the immediate neighbourhood of the limiting point.

For RFSE due to closed trajectories (figure 9*a*) the path from one side of the plate to the other occupies one half of a cyclotron period, but the electron can return to the skin layer many times, so that

$$A \sim e^{-\lambda/l} + e^{-2\lambda/l} + e^{-3\lambda/l} + \ldots = (e^{\lambda/l} - 1)^{-1}$$
$$= [\exp(\pi\nu_{\text{eff}} m_c c/eH_0) - 1]^{-1} \tag{44}$$

where H_0 is the field at which the line is observed. (Equation (44) is valid for two-sided excitation of the plate by an electromagnetic wave, provided the AC electric fields at the surfaces satisfy $\mathscr{E}(0) = -\mathscr{E}(d)$; it is not difficult to write down analogous expressions for other types of excitation.)

Equations (43) and (44) are applicable only when the quasistatic condition

$$\omega \ll \nu_{\text{eff}} \tag{45}$$

is satisfied; the frequency ω of the AC field must be such that the field in the skin layer does not change appreciably over the time the electron moves without being scattered (Haberland and Shiffman 1967). Experiments are usually carried out in the frequency range $\omega/2\pi \approx 10^6$–10^7 Hz, for which this condition is almost always satisfied.

A lower limit on the frequency ω is due to the requirement that δ/d should be small, in fact the need to have a skin layer is the only reason why an AC field is necessary.

4.2.1. Optimal experimental conditions. The temperature dependence of ν_{ph} can thus be deduced from measurements of $A(T)$ by using (43), (44) and (34). It is advantageous to use samples which are as thick as possible, first because an increase in d, and hence in λ which is proportional to d (and a reduction in Ω) increase the sensitivity of the amplitude A to changes in ν_{eff}. Secondly,

$$\exp(-\pi\nu_{\text{eff}}/\Omega) \ll 1 \tag{46}$$

for $\lambda/l > 1$, and even for closed orbits we can use (43) instead of (44); in the former n should be put equal to $\frac{1}{2}$. Equation (43) is much more convenient, since on taking logarithms the term containing ν_{ph} separates, and in coordinates $(\ln A, T^r)$ the experimental points lie on a straight line:

$$\ln A(T) = \text{const} - (2\pi n/\Omega)\beta T^r, \qquad \nu_{\text{ph}} = \beta T^r \tag{47}$$

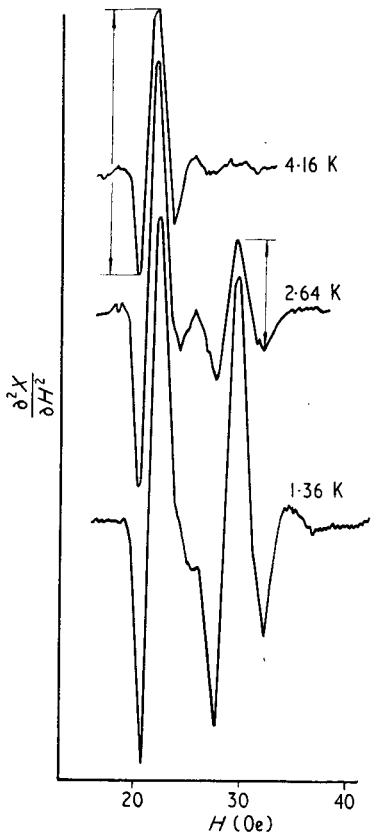

(*a*)

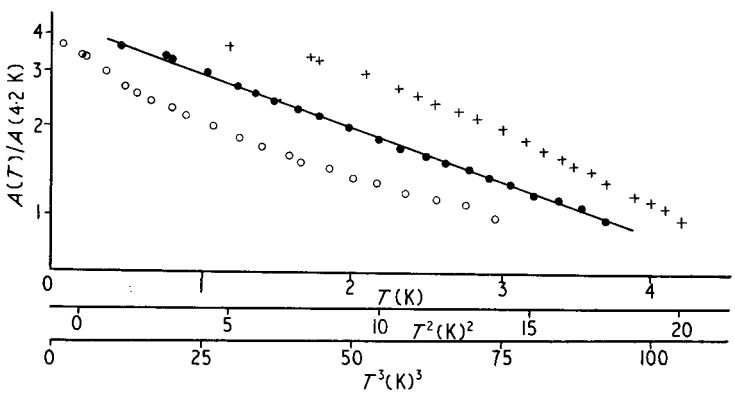

(*b*)

Figure 10. (*a*) Typical traces of RFSE lines for closed trajectories in antimony. The left-hand line is from a hole ellipsoid and the right-hand from an electron ellipsoid. $d = 0{\cdot}32$ mm; $\omega/2\pi = 12{\cdot}5$ MHz. X is the imaginary part of the surface impedance. The amplitudes used for analysis are defined by the arrows. (*b*) Amplitude of the RFSE line from a hole ellipsoid as a function of T (shown by +), T^2 (shown by ●), and T^3 (shown by ○). It can be seen that the filled circles are a good fit to a straight line; β is determined from the tangent of its slope (see equation (47)) (from Gantmakher and Dolgopolov 1971).

(see figure 10(*b*)). If we start from (44), (47) is replaced by the expression

$$\ln\left(\frac{C}{A(T)}+1\right)=\frac{2\pi n}{\Omega}\nu_0+\frac{2\pi n}{\Omega}\beta T^r;\ C=A(0)\left[\exp\left(\frac{2\pi n}{\Omega}\nu_0\right)-1\right] \tag{48}$$

in which, unlike (47), the argument of the logarithm contains the parameter C, which is mainly determined by the value of ν_0.

A useful feature of (47) is that ν_0 and ν_{ph} appear in it in different items. This enables us to determine ν_{ph} when $\nu_{ph}\ll\nu_0$. An increase in sensitivity is needed to satisfy this inequality, but this also ensures that the line shape and the value of δ remain unchanged over the whole temperature range. The point is, that for $\boldsymbol{H}$ parallel to the surface and $\Omega\tau\gg1$ (the condition for electrons to return to the skin layer many times), the value of δ and also the RFSE line width depend on ν_{eff} (Naberezhnykh *et al* 1971) which means that the amplitude measurements $A(T)$ are of little value so long as $\nu_0\approx\nu_{ph}$. If the sample thickness is chosen so that the apparatus is operating near to the limit of sensitivity, then the condition in (46) is automatically satisfied and there are no problems with the temperature dependence of δ.

4.2.2. Size of the effective region. Estimates of the size of the effective region Σ can be obtained either from the general expressions for $\Delta f(x,\boldsymbol{k})$ (Kaner and Gantmakher 1968), or by using simple physical arguments (Tsoi and Gantmakher 1969).

Contributions to the RFSE line come from a certain layer of orbits on the fermi surface which have the same characteristic dimension for the trajectory (to an accuracy of δ). As an example, the width of this layer for an RFSE line from the central section of a spherical fermi surface with radius k_f is

$$\Delta_1 k\approx k_f(\delta/d)^{1/2}. \tag{49}$$

The important electrons within this layer are a group which have a particular phase of rotation in their orbit. It is well known that under the conditions of the anomalous skin-effect the perturbation to the equilibrium distribution function $\Delta f\neq0$ only over a narrow region on the fermi surface. If there is no magnetic field, $\Delta f(x,\boldsymbol{k})\neq0$ only for distances $x\leqslant\delta$ from the surface, and only in a layer of thickness $\Delta k\approx k_f(\delta/l)$ along the line $v_x=0$ on the fermi surface, the 'effective zone' as it is often called. In a magnetic field $\Delta f(x,\boldsymbol{k})$ is non-zero over a much larger distance $x\sim l\gg\delta$, and in particular this gives rise to current splashes within the metal (Kaner and Gantmakher 1968). For any value of x' the perturbation $\Delta f\neq0$ is true only in a narrow zone whose position on the fermi surface depends on x in the same way as that of the corresponding electrons moving over the fermi surface in a magnetic field (see figure 11). The width $\Delta_2 k$ of the zone also depends on x, and both this and $\Delta_1 k$ are functions of the parameter δ/R, where R is the cyclotron radius. For example, for a quadratic dispersion law and a magnetic field H parallel to the surface of the metal, the width of the zone near the central section oscillates

$$\left.\begin{array}{lll}\text{from} & \Delta_2 k^{(1)}\approx k_f(\delta/R)^{1/2} & \text{for } x\approx 2nR\\ \text{to} & \Delta_2 k^{(2)}\approx k_f(\delta/R) & \text{for } x\approx(2n+1)R\end{array}\right\}\quad n=0,1,2,\ldots. \tag{50}$$

In order to apply these estimates to the first RFSE line ($d=2R$), R in these expressions should be replaced by d. For an orbit near a limiting point in an inclined field $\boldsymbol{H}$, $\Delta_2 k$ oscillates from $k_f(\delta/R)^{2/3}\psi^{1/3}$ for $x\approx 2\pi n\psi R$ to $k_f(\delta/R)$ for $x\approx(2n+1)\pi\psi R$ ($n=0,1,2,\ldots$).

For a fermi surface of arbitrary shape the values of k_f in the above estimates would be a little different. The value of $\Delta_1 k$ for a closed extremal orbit is determined by the radius of curvature of the fermi surface at the point $v_x = 0$ on an extremal orbit in a plane containing the magnetic field (see figure 11); the value of $\Delta_2 k$ is determined by the radii of curvature of this orbit at different points.

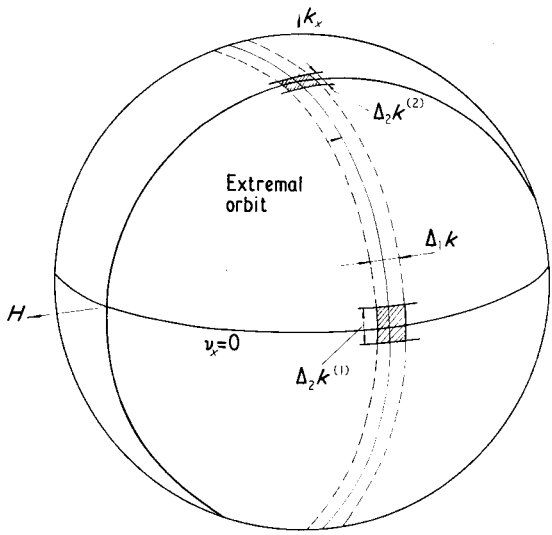

Figure 11. Effective zones Σ for RFSE from an extremal orbit on a spherical fermi surface. The zone Σ for $x = 0, 2R, 4R, \ldots$ is $\Delta_1 k \Delta_2 k^{(1)}$; the zone Σ for $x = R, 3R, 5R, \ldots$ is $\Delta_1 k \Delta_2 k^{(2)}$.

4.2.3. Averaging of the collision frequency along the extremal orbit. Typical experimental values of δ/d lie in the range 10^{-1}–10^{-2}, and at helium temperatures the values of q_T/k_f lie in approximately the same range. Hence q_T can be either greater or less than $\Delta_{1,2} k$. This is in agreement with the fact that the experimentally observed dependences vary from $\nu^*_{ph} \sim T^5$ (figure 12) to $\nu_{ph} \propto T^3$ or T^2 (figures 10 and 13). Moreover, since $\Delta_2 k$ is a function of x, it can happen that the condition in (33) is satisfied over one part of the trajectory but not over the rest. This was clearly the case in the experiments on potassium (Tsoi and Gantmakher 1969, Blaney and Parsons 1970), where the estimate of q_T lies in between the two values in (50). A transition from a cubic dependence to T^4 was observed in these experiments as the sample thickness was reduced, and δ/d correspondingly increased (figure 13).

A comparison of these results for potassium (figure 13) with those for cadmium (Naberezhnykh and Tsymbal 1967) shown in figure 12 is quite instructive. It follows from (49) and (5) that the region of effectiveness is narrower, and hence that small angle scattering is more effective, over the part of the trajectory where the electron moves normal to the surface of the plate. The inset in figure 12 shows the shape of the relevant trajectory in cadmium. It is such that there is no region with $\Delta_2 k \approx \delta/d$, and therefore, despite the approximately equivalent experimental conditions, different temperature dependences were observed: in potassium it was possible to measure the total scattering probability over at least part of the trajectory, but in cadmium the scattering was diffusive over the whole trajectory.

It is clear from figure 11 that the electron–phonon collision frequency measured from the RFSE from a closed trajectory is an average value along the extremal orbit, so that in all the expressions in this section it would be more correct to write instead of ν_{ph} the averaged value

$$\langle \nu_{ph} \rangle = \frac{\hbar}{2\pi m_c} \oint_{\text{orbit}} \frac{dk\, \nu_{ph}}{v_\perp} \tag{51}$$

(the weighting factor $v_\perp^{-1}$ takes into account the rate at which the electron moves around the extremal orbit). We shall, however, omit these brackets wherever this will not lead to ambiguity.

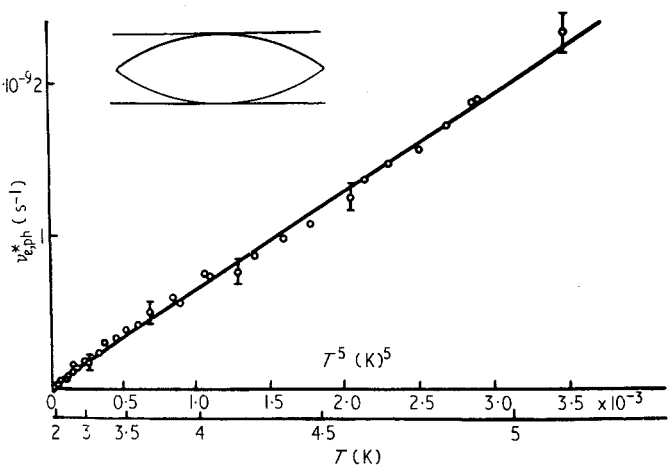

Figure 12. Dependence $\nu^*_{ph}(T)$ for cadmium for a trajectory whose shape is shown in the inset (from Naberezhnykh and Tsymbal 1967).

For (51) to be applicable, the scattering must be effective along the whole trajectory, but we saw from the experiments on potassium that this is sometimes not the case. A second weighting factor, which takes into account the effectiveness of scattering, must then be included in (51). One such factor which might be proposed is, for instance, the cosine of the angle ξ between the electron velocity and the normal to the sample surface

$$\langle \nu_{ph} \rangle = \frac{\hbar}{2\pi m_c} \oint_{\text{orbit}} \frac{\cos\xi\, \nu_{ph}\, dk}{v_\perp}. \tag{52}$$

The amplitude of an RFSE line at a limiting point is determined by scattering over an orbit with diameter $2\psi k_f$ around the limiting point (k_f is the radius of curvature at the limiting point). For small ψ the value obtained for ν_{ph} refers directly to the limiting point, but for large ψ the difference between the limiting point and the extremal orbit around it can become appreciable (Snyder 1971).

4.3. Cyclotron resonance

Azbel'–Kaner cyclotron resonance (CR) occurs at magnetic fields satisfying the condition

$$\omega = n\Omega_n \qquad (n = 0, 1, 2, \ldots). \tag{53}$$

The field in the skin layer changes by an integral number of cycles in the time which the electron takes to go around its orbit and return to the skin layer (Azbel' and Kaner 1958). The time between electron collisions must of course be much greater than the time for one cycle of the electromagnetic field: $\omega\tau \gg 1$.

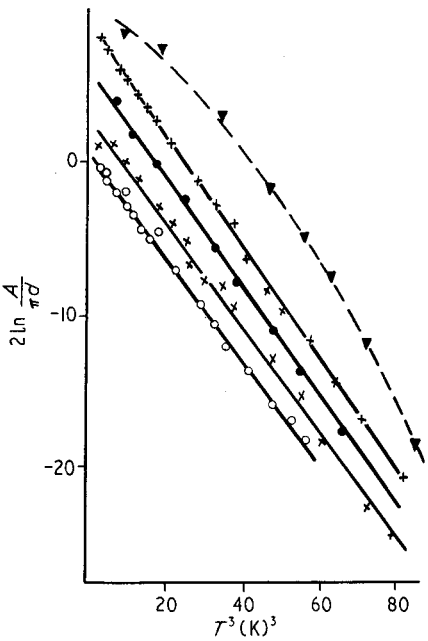

Figure 13. RFSE from an extremal closed orbit in potassium. $\omega/2\pi \approx 4$ MHz: ○—sample thickness 0·63 mm; ×—0·26 mm; ●—0·23 mm; +—0·24 mm; ▼—0·09 mm (from Tsoi and Gantmakher 1969).

The discussion of ν_{ph} in § 4.1 is also valid here for frequencies up to $\omega/2\pi \approx 1{\cdot}5 \times 10^{10}$ Hz at helium temperatures such that $\hbar\omega < T$: the fermi surface has an effective zone with an area of order $\Delta_1 k \Delta_2 k$; when the condition in (33) is satisfied a single collision will remove an electron from this region; and the measured collision frequency is related to the matrix element in (5) by (39)–(41). In cyclotron resonance it is probably not necessary to take into account the magnetic field variation of the collision frequency ν_{ph} for an electron near an extremal section (see equations (25) and (27)), because the width $\Delta_1 k$ of the effective region is usually much greater than the value of k_z given by (21).

4.3.1. Size of the effective zone. The values of $\Delta_1 k$ and $\Delta_2 k$ are of course different from those in RFSE.

The thickness $\Delta_1 k$ of the layer of resonant orbits depends on the dispersion of the cyclotron mass. If the mass of all orbits is the same, then all orbits are in resonance together. If $m_c = m_c(k_z)$, the relative width of the resonance is $\Delta H_n/H_n \sim \Delta m_c/m_c$ and also $\Delta H_n/H_n \approx (\omega\tau)^{-1}$ (Azbel' and Kaner 1958, Chambers 1965), so the thickness of the resonant layer is

$$\Delta_1 k \approx \left(\frac{m_c}{\omega\tau}\right)^{1/2} \left(\frac{\partial^2 m_c}{\partial k_z^2}\right)^{-1/2}. \tag{54}$$

However, the other dimension $\Delta_2 k$ of the effective zone is usually more important from the point of view of the effectiveness of collisions, and this is determined by the time which an electron spends in the skin layer ie we usually have $\Delta_2 k \leqslant \Delta_1 k$. This dimension, as in RFSE, changes along the orbit in accordance with (50). Where the electron is moving parallel to the surface of the metal and scattering leads only to a reduction in the phase of rotation, $\Delta_2 k^{(1)} \approx k_2(\delta/R)^{1/2}$; but where the electron is moving perpendicular to the surface a more important consequence of the scattering is a shift in orbit centre, and $\Delta_2 k^{(2)} \approx k_f(\delta/R)$. The numerical value of δ/R in cyclotron resonance is of the same order of magnitude as in RFSE, ie both δ and $R \propto H^{-1}$ are 20–30 times smaller in CR than in RFSE. This means that the temperature dependences observed experimentally in CR can also be as T^5, T^3 or T^2.

The fact that $\Delta_1 k$, and hence the number of resonant electrons, depends on τ, must in general affect the CR amplitudes. This dependence explains why Kaner and Azbel' (1957) obtained different power laws for the temperature dependences of the CR amplitudes for quadratic and nonquadratic dispersion laws. However, the expressions in this paper were derived on the basis of two assumptions. Firstly, it was assumed that resonant electrons make the main contribution to the impedance, so that the penetration depth δ changes appreciably at resonance, and secondly, it was assumed that $\nu_0 \ll \nu_{ph}$, so that a change in ν_{ph} changes $\Delta_1 k$, which in its turn changes δ and so on. It is clear that neither of these assumptions is fulfilled experimentally, and therefore the dependences predicted by Kaner and Azbel' have not so far been observed.

4.3.2. Methods of measuring the scattering frequency. The summary frequency ν_{eff} and not ν_{ph} has always been measured in CR experiments, and measurements have been made in two ways. Haüssler and Welles (1966) based their method on the impedance expression

$$Z(H) = Z(0)(1 - e^{-w})^{1/3}, \qquad w = \frac{2\pi}{\Omega}(i\omega + \nu_{eff}) \tag{55}$$

and by differentiating this with respect to H it is straightforward to show that, when the magnetic field derivative of the resonance is measured experimentally, the amplitude of the nth CR line ($\Omega_n = \omega/n$) is given by

$$A_n \sim n^2 \exp(-2\pi n \nu_{eff}/\omega) \tag{56}$$

provided that

$$2\pi n \nu_{eff}/\omega \gg 1. \tag{57}$$

It is now possible to determine ν_{eff} by constructing a graph of $\ln(A_n/n^2)$ as a function of n, and measuring the slope of the straight line obtained when n is sufficiently large (see figure 14).

Although (55) assumes that the impedance is mainly determined by resonant electrons, (56) is also valid in the opposite limiting case when the contribution of resonant electrons is small. This can easily be shown, for instance, by using the ineffectiveness concept (Heine 1957): from the expression for the effective conductivity

$$\sigma_{eff} = \delta\left(a_0 + \frac{a_1}{1 - e^{-w}}\right), \qquad a_0 \gg a_1$$

it follows that

$$Z \sim \left(a_0 + \frac{a_1}{1-\mathrm{e}^{-w}}\right)^{-1/3} \sim 1 - \frac{a_1}{3a_0}(1-\mathrm{e}^{-w})^{-1}. \tag{58}$$

On differentiation with respect to H, this expression again gives (56) provided that (57) is satisfied.

This method has been used to measure $\nu_{\mathrm{eff}}(T)$ both under conditions such that (33) is satisfied (Haüssler and Welles (1966) found that $\nu_{\mathrm{ph}} \propto T^3$ for copper), and in the diffusion limit (Poulsen and Datars (1970) found that $\nu^*_{\mathrm{ph}} \propto T^{4\cdot8}$ for mercury).

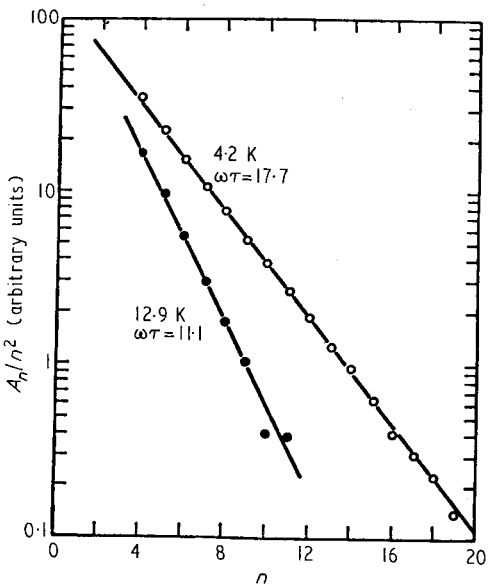

Figure 14. Graphs illustrating the applicability of equation (56) to CR from a central section in copper for $\boldsymbol{H} \parallel [100]$. $\omega/2\pi = 34{\cdot}8 \times 10^9$ Hz (from Haüssler and Welles 1966).

However, this approach can be used only when $\omega\tau$ is not too large; the inequality $2\pi n \gg \omega\tau$ must be satisfied for (56) to be valid, but for n very large the time the electron takes to pass through the skin layer becomes comparable with the period of the microwave field and (56) is again no longer applicable (see §4.3.3 below for a discussion of the retardation effect). Under diffusion conditions $q_{\mathrm{T}} < \Delta_{1,2}k$, there is yet another difficulty in the interpretation of results, specifically related to the electron–phonon part of the scattering frequency: both $\Delta_2 k$ and the effective frequency $\nu^*_{\mathrm{ph}} \approx \nu_{\mathrm{ph}}\,(\Delta_2 k/q_{\mathrm{T}})^2$ can vary with the resonance number.

Both these difficulties in the measurement of ν_{ph} can be avoided by slightly changing the method of measurement: by fixing the number of the resonance one can use (56) to analyse the dependence $A_n(T)$, exactly as was done for the RFSE (cf (43); in distinction from (43) it is not assumed in (56) that the electron returns to the skin layer once only). Just as in RFSE, the inequality $\nu_{\mathrm{ph}} \ll \nu_0$ does not reduce the accuracy of measurements of ν_{ph}, but in fact increases their reliability, because this inequality ensures that $\Delta_2 k$, δ and the resonant factor in equations (55) or (58) are independent of temperature. No measurements of $A_n(T)$ for fixed n have so far been published.

The second method of determining ν_{eff} is based on an analysis of the CR line shape. It was shown by Chambers (1965) that when an electron makes a sufficiently

large number of revolutions within its mean free time ($\omega\tau \gtrsim 50$), but at the same time the impedance is determined mainly by nonresonant electrons, the line shape becomes independent of τ and is basically determined by the derivative $(\partial^2 m_c/\partial k_z^2)$ ie by the dispersion of the cyclotron mass. The line width then depends only on $\omega\tau$ (the ratio between the number of resonant and nonresonant electrons is in fact not at all critical (Goy and Weisbuch (1969)). The first measurements of ν_{ph} from the CR line width were made by Moore (1966) on gallium, who found that $\nu_{ph} \propto T^3$ (figure 15).

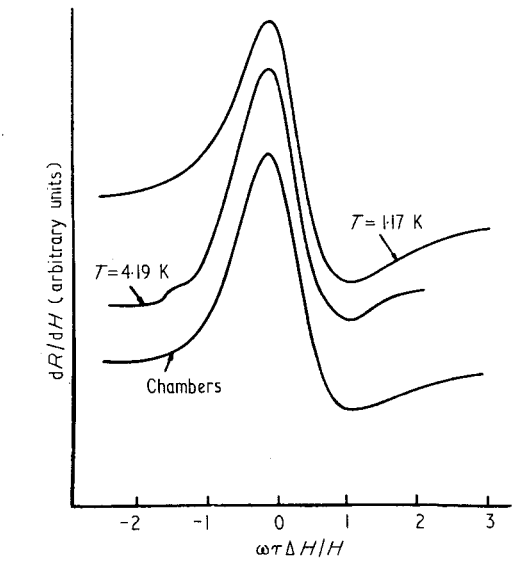

(*a*)

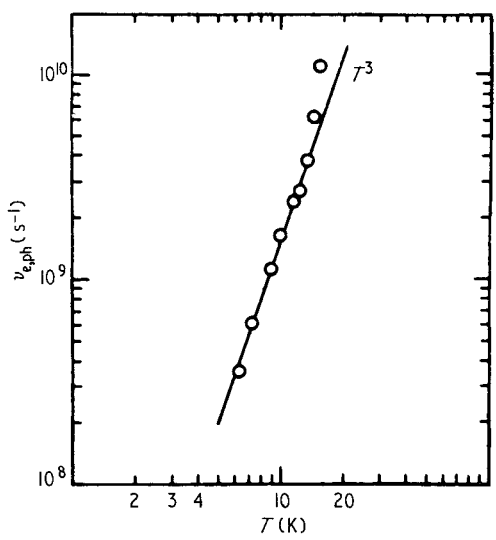

(*b*)

Figure 15. (*a*) Comparison of experimental CR line shape in gallium (two upper curves) with calculated line shape. $\omega/2\pi = 3{\cdot}7 \times 10^{10}$ Hz; H parallel to a axis. (*b*) Dependence $\nu_{ph}(T)$ derived from the line widths (from Moore 1966).

The fact that $\omega\tau \gg 1$ means that all the measurements of both CR line amplitudes and widths take place under conditions such that an electron returns repeatedly to the skin layer. Therefore, if one is not just observing CR in order to determine the cyclotron mass, but is using it to measure ν_{eff}, it is necessary to orient the magnetic field parallel to the sample surface with great accuracy, as otherwise electrons will fail to return to the skin layer, not because they are scattered but because they have a drift velocity along the field. The necessary accuracy is sometimes of the order of 1′ or even better (Moore 1966, Poulsen and Datars 1970). The same rigorous demands also apply, of course, to the surface of the sample itself.

4.3.3. Retardation effect. The effect of retardation was mentioned above: the amplitude and line shape of CR are affected by the change in phase of the high-frequency field during the passage of an electron through the skin layer. The parameter η which characterizes this effect is the square of the ratio of the time an electron spends in the skin layer $(R_n\,\delta)^{1/2}/v$ to the period of the high-frequency field ω^{-1} (Drew 1972):

$$\eta = R_n\,\omega^2\,\delta/v^2. \tag{59}$$

It increases with increasing frequency as $\eta \sim \omega^{2/3}$ (since $\delta \sim \omega^{-1/3}$ and $R_n \propto \omega^{-1}$ for fixed n) and becomes comparable with unity at frequencies of 10^{12}–10^{13} Hz. The presence of retardation effects gives rise to an additional exponential factor of the type e^{η} in the expression for the impedance in (55) and also changes the line shape. It is possible for the CR amplitude and line shape to be determined mainly by retardation effects and not by a finite relaxation time (Drew and Strom 1970).

The cyclotron mass in (20) is an average property of an orbit, but the quantities R_n and v in (59), which determine the time an electron takes to pass through the skin layer, refer just to the neighbourhood of the effective point $v_x = 0$ on an extremal orbit. It follows that when the shape of the trajectory is unfavourable retardation effects can occur at much lower frequencies $\omega \approx 10^{10}$–10^{11} Hz. This was shown experimentally for CR lines in gallium and indium by Kamgar *et al* (1972).

4.3.4. Cyclotron resonance at high frequencies. Retardation effects are not the only difficulty which arises in the interpretation of CR experiments at high frequencies. The photon energy $\hbar\omega \approx 10$ K even at a frequency $\omega/2\pi \approx 2 \times 10^{11}$ Hz, and this means that in CR at frequencies 10^{11}–10^{12} Hz an electron changes its energy by an amount greater than T.

Under these conditions (39)–(41) cannot be used. The energy level scheme for CR at the fourth harmonic ($n = 4$) and $\hbar\omega \gg T$ is shown in figure 16. The heavy lines on the parabolas corresponding to (19) show the electron states from which upward transitions due to the electromagnetic field can take place. Since the range of variation of α is large for these states, from 1 to $-(\hbar\Omega/T + 1)$, the linear method of averaging the value of ν, described in §4.1, is clearly no longer applicable. Instead, we can use the following approach. The width of the resonant line at transitions is determined by the sum of the widths of the upper and lower levels taking part in the resonance. Since the collision frequency ν_{ph} is described by the symmetrical curve $\mathscr{T}_2(\alpha)$ (see figure 8), this sum has a minimum when the upper and lower levels are symmetrically situated with respect to E_{f}. The corresponding states of the lower level are shown by small circles in figure 16; they lie at the intersection of the parabolas with the lines $E_{\text{f}} - E = \hbar\omega/2$. It is natural to assume

that these electrons make the main contribution to CR and determine the experimentally observed line width (Cheremisin 1972).

It is now possible to analyse the experimental results by using the expression

$$\nu_{\mathrm{ph}}^{(\omega)} = \frac{1}{4\pi}\frac{\Delta^2 T^3}{\hbar^4 \mu s^4 v}\mathscr{T}_2\left(\frac{\hbar\omega}{2T}\right) \tag{60}$$

which tends to (16) for $\omega \to \infty$. Since $\mathscr{T}_2(\alpha)$ approximates its asymptotic value $\alpha^3/3$ only for $\alpha \approx 10$, the temperature dependence of $\nu_{\mathrm{ph}}^{(\omega)}$ is preserved to quite large

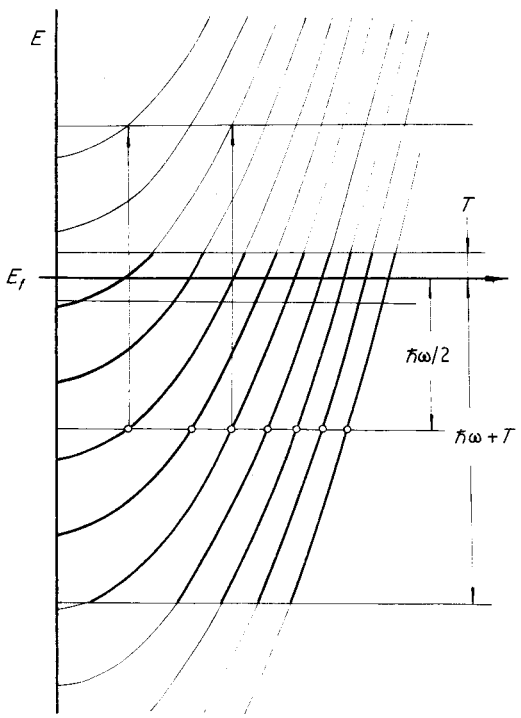

Figure 16. Energy level scheme for CR at high frequencies ($\hbar\omega \gg T$, $\omega/\Omega = 4$).

values of ω. In particular, and in agreement with the experimental results of Goy and Castaing (1973), shown in figure 17,

$$[\nu(3{\cdot}8^\circ) - \nu(1{\cdot}5^\circ)]_{\hbar\omega=22^\circ} = 1{\cdot}5[\nu(3{\cdot}8^\circ) - \nu(1{\cdot}5^\circ)]_{\hbar\omega=13^\circ}.$$

4.4. Ultrasonic absorption

A sound wave produces a periodic perturbation to the crystal lattice, which propagates with velocity $\boldsymbol{s}$ along the sound wave vector $\boldsymbol{p}$. Electrons moving in the field of the wave can take energy from it and therefore attenuate it. At low temperatures, when the electron mean free path becomes greater than the sound wavelength $\Lambda = 2\pi/p$, electron damping becomes dominant. In this case, as in the anomalous skin effect, there is a Landau damping mechanism: energy is mainly acquired by those electrons which are moving in phase with the wave ie those whose velocity $\boldsymbol{v}$ satisfies the equation

$$\boldsymbol{v}.\boldsymbol{p} = \omega. \tag{61}$$

Since the sound frequency $\omega = ps$, but $s \ll v$, (61) means that $\boldsymbol{v} \perp \boldsymbol{p}$. We again find ourselves with an 'effective zone' on the fermi surface, but this time along the line $\boldsymbol{v}.\boldsymbol{p} = 0$. In the absence of a magnetic field the width of this zone is of order $k_f(pl)^{-1}$. In the presence of a field an electron interacts with the wave only in those parts of its orbit which are near the intersection with this line. There can be several such intersection points on an orbit, and the resulting interaction of an electron with the wave depends on the phase relation of the sound wave at all the effective points of the electron trajectory. Since the dimensions of this trajectory, the cyclotron frequency and the phase relation are all functions of H, the contribution of each orbit to the absorption varies with the magnetic field. As always happens in such cases, both oscillations and individual lines in the absorption are determined by orbits with extremal parameters.

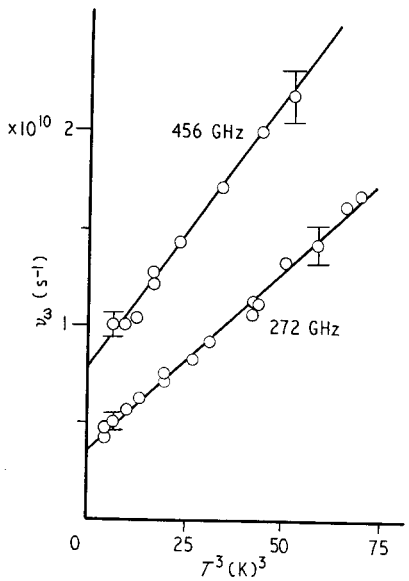

Figure 17. CR in lead: frequency $\nu_{ph}^{(\omega)}$ as a function of T^3 at two different frequencies (from Goy and Castaing 1973).

There is a considerable number of oscillatory effects in the ultrasonic absorption, due to particular groups of extremal orbits. It is clear from the above that the methods of measuring ν_{ph} from these effects are basically similar to the electrodynamic methods which have been discussed in the last two sections.

4.4.1. Geometric oscillations. The best known and most widely studied effects are the geometric oscillations in the ultrasonic absorption. Each new cycle of these oscillations corresponds to a value of the field H for which a characteristic dimension of the electron trajectory is an integral multiple of the sound wavelength (Pippard 1960). It is not difficult to see an analogy between this effect and the RFSE. The quantity $n\Lambda$ ($n = 1, 2, 3, \ldots$) corresponds to the plate thickness, and the distance over which the phase of the wave varies appreciably, which is approximately $\Lambda/\pi = 2/p$, corresponds to the thickness δ of the skin layer; hence the estimates in (49) and (50) for the dimensions of the region Σ become, when expressed in terms

of the cyclotron radius, $R_n = n\Lambda/2$,

$$\Delta_1 k \approx k_f(pR)^{-1/2}; \quad \Delta_2 k^{(1,2)} \approx k_f(pR)^{-1/2},\ k_f(pR)^{-1}. \tag{62}$$

The quasistatic condition in (45) remains the same; it follows from it that $\omega \ll \Omega$, since $\Omega/\nu \geqslant 1$. If the condition in (46) that the electron does not go round the orbit more than once is also satisfied, then the ultrasonic absorption coefficient for a quadratic dispersion law is proportional to (Phua and Peverley 1971)

$$\alpha_s \sim 1 + 2(\pi pR)^{-1/2} \exp(-\pi\nu_{\text{eff}}/\Omega) \sin(2pR - \pi/4). \tag{63}$$

The first factor in the oscillatory term is the width of the layer of effective orbits $\Delta_1 k/k_f$, which is already well known to us, and the second factor, which we have also met before, is the probability that an electron passes, without being scattered, from one effective point on the orbit to another.

All the discussion of the physical interpretation of ν_{ph} in previous sections is also applicable here; in particular (39)–(41) are valid when the condition in (33) is satisfied.

Measurements of ν_{ph} from the amplitudes of geometric oscillations of sound attenuation were reported by Phua and Peverley (1971); the total scattering frequency ν_{eff} was determined from the amplitude variation of the sinusoids at a fixed temperature by plotting $\ln(An^{1/2})$ against n (see figure 18; cf (56) and figure 14). A dependence $\nu_{\text{ph}} \propto T^3$ was found for copper, but with a coefficient rather less than that obtained by other methods. The difference is probably because the inequality in (33) was only just satisfied. It is appropriate here to make the same observation as in the preceding section: (63), which is similar to (56), enables us to analyse measurements of $A(T)$ for a fixed oscillation number, and derive ν_{ph} directly. This can be a useful check on the results obtained.

4.4.2. Geometric resonance from open trajectories. Just as in RFSE electron trajectories of various types can give rise to observable features in the sound absorption. The effect being due to open trajectories the harmonic oscillations are replaced by a series of narrow maxima in the absorption at fields

$$H_n = Kpc \sin\psi_0/2\pi ne \qquad (n = 1, 2, 3, \ldots) \tag{64}$$

(a reciprocal lattice vector K appears in (64) instead of k_f; ψ_0 is the angle between $\boldsymbol{p}$ and the open direction). It was shown by Kaner *et al* (1961) that the relative width of these maxima is

$$\Delta H/H = \pi/pl. \tag{65}$$

The spatial resonance occurs over a field range such that over a distance l the difference between $n\Lambda$ and the displacement of the electron along $\boldsymbol{p}$ in a cyclotron period, $\Delta K = Kc \sin\psi_0/He$, is not distinguishable. However, the size of the region Σ does not depend on the parameter pl: the dimension $\Delta_1 k$ is simply the width of the layer of open orbits which have effective points $\boldsymbol{p}.\boldsymbol{v} = 0$; and $\Delta_2 k$ is determined by (62). If the effective point is a point of inflexion on the open trajectory (similar to the effective points on the trajectory shown in figure 9(*b*)), then R, which is essentially the second derivative of the curve $x(y)$ describing the trajectory, is replaced by the third derivative in the expression for $\Delta_2 k$: $\Delta_2 k \approx (eH/\hbar c)(px''')^{-1/3}$.

This effect has been used to measure collision frequencies in cadmium (Deaton and Gavenda 1964); they found that $\nu^*_{\text{ph}} \propto T^4$, which shows that the condition in

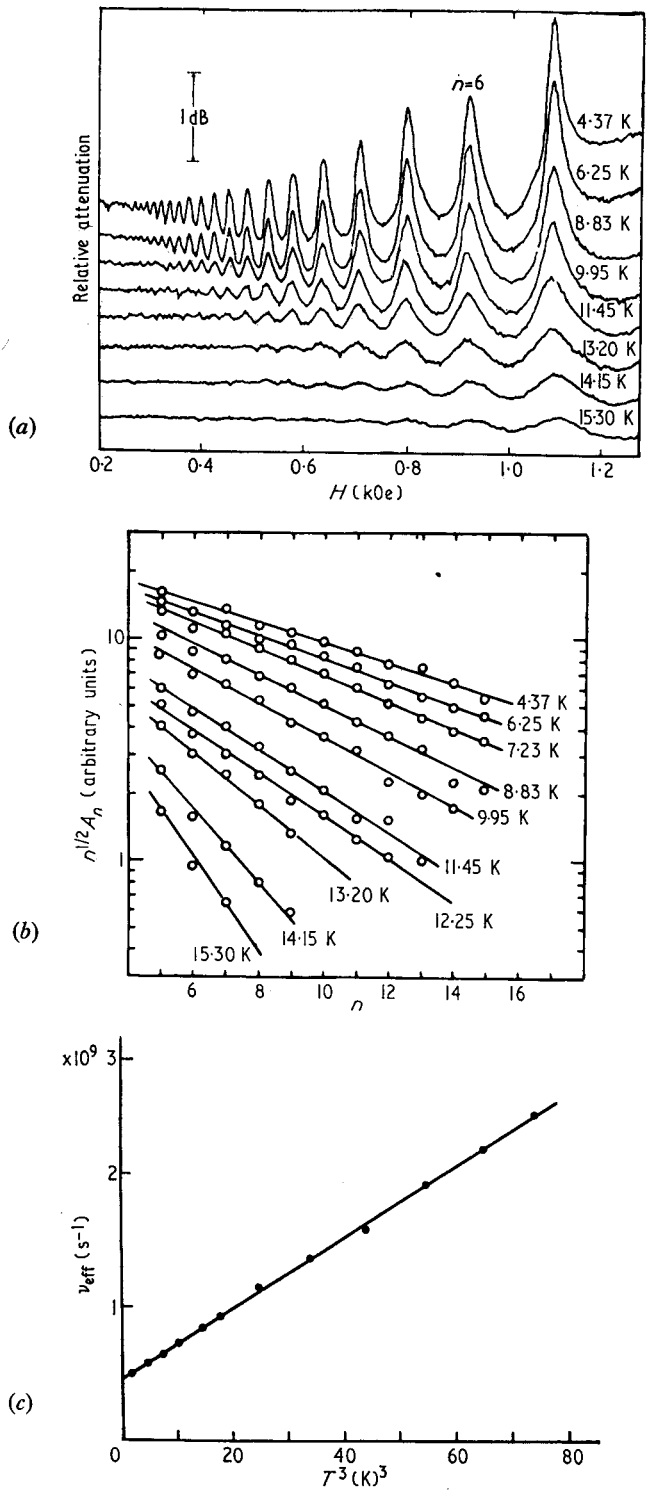

Figure 18. (*a*) Magnetoacoustic oscillations in copper for $\boldsymbol{p} \parallel [110]$ and $\boldsymbol{H} \parallel [001]$. $\omega/2\pi =$ 165 MHz. (*b*) Analysis of this data, using equation (63). A is the amplitude of the oscillations. (*c*) Dependence $\nu_{\mathrm{ph}}(T)$ (from Phua and Peverley 1971).

(33) is violated. (In a later publication (Deaton 1965) it is stated that the dependence $\nu_{ph} \propto T^3$ was also observed.)

Electron scattering can be studied not only by spatial resonances, but also by using space–time resonances such as Doppler-shifted acoustic CR (Stark *et al* 1971), but this possibility has been little studied.

In general ultrasonic absorption also presents other possibilities for the study of the electron–phonon interaction, since the deformation potential $\tilde{\Delta}$ enters directly into the absorption coefficient, rather than through factors containing ν_{ph} as in (63). This enables, for example, particular components of the tensor $\tilde{\Delta}$ to be determined from measurements of the amplitude of giant quantum oscillations in the sound absorption (Walther 1968). However, a discussion of these topics would lead us too far from the subject of this review.

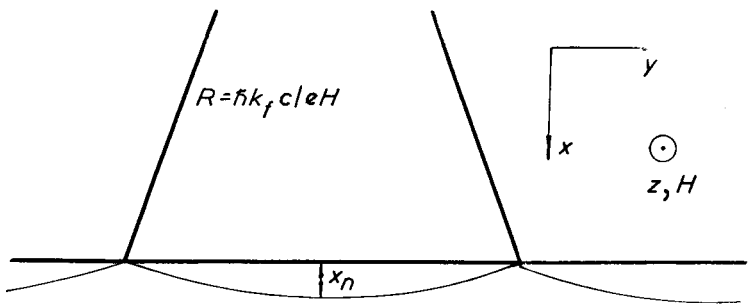

Figure 19. Shape of the classical trajectory corresponding to magnetic surface levels.

4.5. *Magnetic surface levels*

Near the surface of a metal in a weak magnetic field there exist magnetic surface levels, associated with electrons skipping along the surface with successive reflections from it (eg see the review of Khaikin 1968). For a quadratic dispersion law the energy spectrum of these electrons has the form (Nee and Prange 1967)

$$E_n(k_y, k_z) \approx \frac{\hbar^2 k_y}{2m} + \frac{\hbar^2 k_z}{2m} + \left(\frac{3\pi}{2}\right)^{2/3} \left[\frac{\hbar^2 k_y^2}{2m} (n\hbar\Omega)^2\right]^{1/3}, \quad n = 1, 2, 3, \ldots \tag{66}$$

(for simplicity we do not distinguish here between the cyclotron and the band masses, putting $m^* = m_c = m$; the coordinates are as shown in figure 19; k_y is related to the x coordinate of the orbit centre, which is outside the metal). When an electromagnetic wave of frequency ω satisfying the condition

$$\omega = \omega_{ij} \approx \left(\frac{3\pi}{2}\right)^{2/3} \left(\frac{\Omega^2 E_f}{\hbar}\right)^{1/3} (n_i^{2/3} - n_j^{2/3}) \tag{67}$$

is incident on the metal, resonant transitions conserving k_y and k_z take place between the levels, and these can be observed as narrow lines in the impedance. In essence the effect is analogous to cyclotron resonance, with the difference that it takes place atm uch lower magnetic fields of 1 to 10 Oe. The condition $\omega_{ij}\tau \gg 1$ that these lines can be observed has the usual meaning: the separation of levels must be much greater than their width. This width is determined not only by the usual electron scattering mechanisms—by impurities, lattice defects and phonons—but also to a considerable extent by the coefficient of specular reflection γ of electrons at the surface. For diffusive reflection ($\gamma = 0$) we would have $\omega_{ij}\tau \approx 1$, so the

observation of narrow lines (see figure 20) means that $\gamma \approx 1$ for such small angles of incidence. In general γ can be temperature dependent (Gaidukov and Kadletsova 1970), but, judging from the results of Koch and Doezema (1970), this dependence is unimportant for skipping electrons.

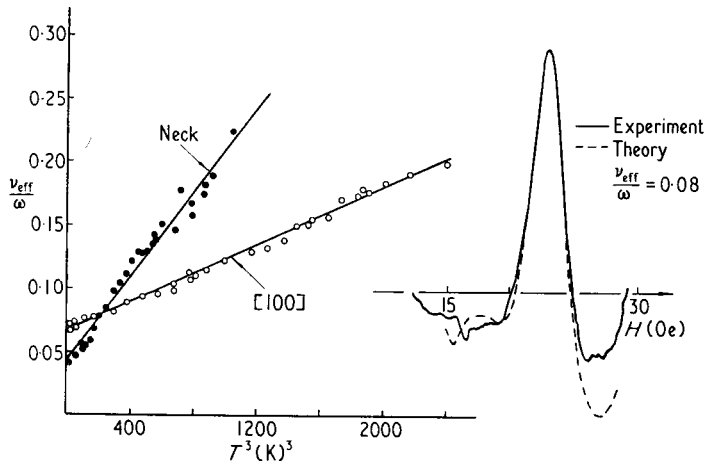

Figure 20. Dependence $\nu_{ph}(T)$ for the neck and for the [100] point on the copper fermi surface. $\omega/2\pi = 3{\cdot}6 \times 10^{10}$ s^{-1}. To the right: a comparison between experimental and theoretical values of $\partial R/\partial H$ at 6·6 K for the transition ω_{12} (R is the real part of the impedance); the zone Σ is in the neighbourhood of the [100] point of the fermi surface (from Koch and Doezema 1970).

The mean distance from the surface of the electrons in which we are interested is

$$X_n = \left(\frac{n^2\hbar c}{ek_f H}\right)^{1/3} \tag{68}$$

which is much greater than the wavelength of a thermal phonon $2\pi/q_T$ even at 1 K. We may therefore expect that the proximity of the metal surface does not affect collisions with phonons and that the temperature broadening of the quantum levels is due to collisions with phonons in the volume of the metal (Koch and Doezema 1970).

The effective collision frequency is therefore now made up of three terms

$$\nu_{eff} = \nu_0 + \frac{1}{2\pi}\omega_{ij}(1-\gamma) + \nu_{ph} \tag{69}$$

of which only ν_{ph} is temperature dependent. This enables us to measure ν_{ph} from the temperature dependence of the resonance line width (see figure 20).

The dimension $\Delta_1 k$ of the effective zone is determined by the dispersion of the parameter $(k_\perp/v_\perp)^{1/2}$ along the line $v_x = 0$ in the region of its extremum (the subscript $\perp$ means that $\boldsymbol{k}$ and $\boldsymbol{v}$ are resolved perpendicular to the vector $\boldsymbol{H}$). This parameter appears in an expression like (54) instead of m_c. The dimension $\Delta_2 k$ is given by the arc length of the electron orbit: $\Delta_2 k \approx k_f(x_n/R)^{1/2}$.

In the experiments on copper referred to above the angular dimensions $\Delta_1 k$ and $\Delta_2 k$ were estimated to be 6° and 0·5°, respectively. In this case, unlike that shown in figure 11, the effective zone Σ does not shift along the fermi surface, because the values of ν_{ph} obtained are averaged only over the small area $\Delta_1 k \Delta_2 k$.

In this sense, only RFSE and CR from limiting points can rival resonance at surface levels. In practice, however, RFSE can rarely be observed for angles $\psi \lesssim 5°$ (it is only for tin that RFSE lines from limiting points have been observed down to $\psi \approx 2°$). In limiting point CR the dimensions of the effective region around the limiting point are determined by the dispersion of the cyclotron mass:

$$\Delta_1 k = k_f^{1/2}\left(\frac{m_c}{\omega\tau}\right)^{1/4}\left(\frac{\partial^2 m_c}{\partial k_z^2}\right)^{-1/4}$$

This effect has never been studied with the aim of deriving information about ν.

The physical interpretation of the parameter ν_{ph}, as determined from resonance at surface levels, follows the discussion in the section on CR, except that Ω_n is replaced by ω_{ij}. The discreteness of the electron spectrum can be neglected in calculations of transitions due to collisions with phonons, provided

$$\hbar\omega_{ij} \ll T^{3/2}(ms^2)^{-1/2}.$$

If we also have $\hbar\omega_{ij} < T$ and the conditions in (33) are satisfied, then (39)–(41) can be used.

5. Landau quantum oscillations

Of all the methods of studying the shape of the fermi surface which are based on distinguishing groups of electrons with extremal values of some parameter, the best known and most widely used method is based on a group of effects which we may combine under the generic name of Landau quantum oscillations. When the spectrum is quantized by a high magnetic field H, the thermodynamic and kinetic properties of a metal are oscillatory functions of the magnetic field, as a consequence of the fact that the electron Landau levels for sections of extremal area empty successively as they pass through the fermi level. The period of the oscillations is determined by the area of the extremal section of the fermi surface, whilst in the simplest case their amplitude has the form

$$A \sim G(H, T)\exp\left[-\frac{2\pi^2(T+W)}{\hbar\Omega}\right] \tag{70}$$

where the parameter W, called the Dingle temperature, is related to the effective collision frequency ν_{eff} by

$$W = \hbar\nu_{eff}/2\pi \tag{71}$$

and the pre-exponential factor $G(H, T)$ is a known function of powers of T and H (eg see the review by Gold 1969).

Recently quantum oscillations have been used more and more for the measurement of relaxation times. The potential of these measurements has been discussed in detail by Springford (1971), although his review is concerned mainly with scattering at impurities. This is not accidental. It is clear from (70) that in general quantum oscillations are not very convenient for investigation of the temperature dependence of relaxation times, since the dependence $A(T)$ is mainly determined by the factor $\exp(-2\pi^2 T/\hbar\Omega)$ which does not contain the relaxation time. However, an attempt was made by Palin (1972) to measure the temperature dependence of W for mercury from the oscillations of magnetic susceptibility (the de Haas–van Alphen effect). The experiments showed that over the temperature interval

from 1 K to 17 K there was no observed deviation from a linear dependence of $\ln(A/G)$ on T (see figure 21); the slope of graphs of $\ln(A/G)$ versus $1/H$ also varied linearly with temperature. This appears to show that W is independent of temperature.

The absence of any dependence $W(T)$, which was found experimentally by Palin, was explained theoretically by calculations of the oscillatory magnetization of a system of electrons interacting with phonons (Englesberg and Simpson 1970). It is known that the electron–phonon interaction leads to a renormalization of the effective mass, and the renormalization coefficient appears, via Ω, in the argument of the exponential which determines the amplitude of oscillations. The result of the calculations can be interpreted as follows: the effect of a change in the scattering probability with temperature ie a change in the imaginary part of the self-energy of particles in the electron–phonon system, is compensated in (70) by the change with temperature of the effective mass (the real part of the self-energy), which enters in (70) through Ω.

Strictly speaking, this result applies only to mercury, since the last step in the calculations was made numerically, using the parameters for this metal. It is worth noting that both mercury and lead are metals which contain low-lying phonon branches. Moreover, the calculations of Englesberg and Simpson refer only to oscillations of thermodynamic quantities, whilst the kinetic parameters of a metal also oscillate with magnetic field. It is not clear beforehand whether a similar compensation will take place in, for instance, the Shubnikov–de Haas oscillations in electrical resistivity.

In this connection it is worthwhile to consider the 'traditional' approach to this problem, which is based on the idea that the Dingle temperature represents the collision broadening of a Landau level, and which does not take into account mass renormalization or its temperature dependence.

We limit ourselves here to some qualitative remarks, based on (25).

The electrons primarily responsible for oscillations are those which lie on a Landau level at the moment it passes through the fermi level ie those electrons with k_z satisfying (22). The collision frequency for these electrons is given by (25), since (23), which is the condition for the existence of a region with $\nu_{\rm ph}$ proportional to H, is practically the same as the condition $\hbar\Omega \gtrsim 2\pi^2 T$ that quantum oscillations can be observed (because $m^* s^2 \approx 0{\cdot}1$ K); at the same time we have $k_z < q_{\rm T}$ for all these electrons, because at helium temperature $T > m^* s^2$.

The variation $\nu_{\rm ph} \sim \Omega T^{3/2}$ enables us to explain the results of Palin (1972). Because $\nu_{\rm ph} \sim H$, the field H cancels out in the argument of the exponential $\exp(-2\pi^2 W_{\rm ph}/\hbar\Omega)$, so that electron collisions have no effect on the slope of the linear dependence of $\ln(A/G)$ on H^{-1} (we are assuming that the Dingle temperature is of the form $W = W_0 + W_{\rm ph}$; cf (34)). Hence the only hope of determining $W_{\rm ph}$ is from the dependence $A(T)$. However, if $W_{\rm ph}$ were directly proportional to T, the dependence of $\ln(A/T)$ on T would still be linear and collisions with phonons would lead merely to a small change in the slope of the straight line, equivalent to a renormalization of the effective mass. Hence, any deviation expected from a linear dependence of $\ln(A/G)$ on T is due to the difference from unity of the exponent of the temperature in (25), and this difference is very small.

From the estimate given by Palin we would expect $W_{\rm ph} \approx 0{\cdot}4°$ at $T = 4$ K and by assuming that $W_{\rm ph} \propto T^{3/2}$ we can plot values of $2\pi^2 W_{\rm ph}/\hbar\Omega$ below the experimental points of the lower curve ($H = 20$ kOe) in figure 21. It is clear that the crosses thus

obtained fit a straight line as well as do the initial points. This means that the experimental accuracy is not sufficient to determine the expected deviations from linearity.

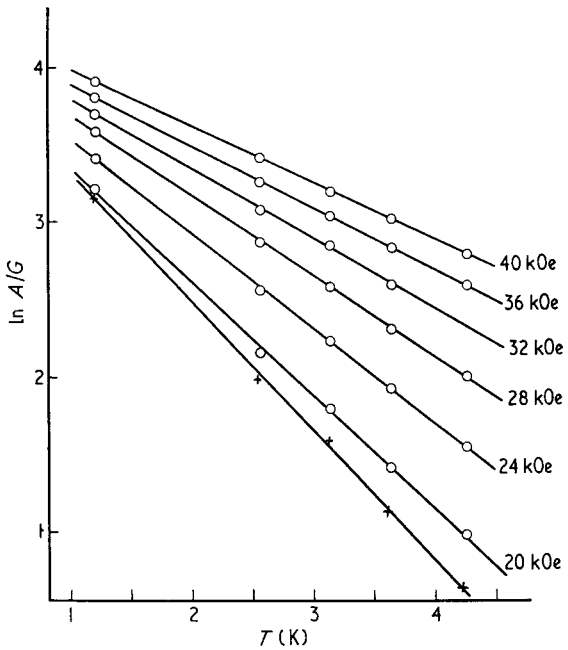

Figure 21. Graphs of the temperature dependence of the β oscillations in mercury. The size of the circles gives a rough idea of the experimental errors. The value of the magnetic field in kOe is shown by each straight line (from Palin 1972). The result of subtracting $2\pi^2 W_{\rm ph}/\hbar\Omega$, varying as $T^{3/2}$ ($W_{\rm ph}$ (4K) = 0·4 K), from the experimental points of the lowest line is shown by +.

The observation of these collisions from the amplitude of quantum oscillations is thus a very difficult experimental problem, despite the fact that for an extremal section of the fermi surface in a high magnetic field the frequency of electron–phonon collisions $\nu_{\rm ph}$ is $(\hbar\Omega)(m^* s^2)^{1/2} T^{-3/2}$ times greater than in the absence of a field (the dependence in (25) instead of the usual T^3).

6. Experimental results

In conclusion we carry out a brief review of the presently available experimental results for the electron–phonon scattering probability in metals. In this we have in mind the total scattering probability referring to well defined regions of the fermi surface, so that we shall discuss only results obtained from kinetic effects referring to extremal trajectories. The results of these experiments in which it was possible to satisfy the condition in (33) and obtain a value of $r \leqslant 3$ in the temperature dependence $\nu_{\rm ph} = \beta T^r$ are collected in tables 1 and 2.

6.1. Quadratic dependence of $\nu(T)$

6.1.1. Bismuth. When the dependence $(\nu_{\rm eff} - \nu_0) \sim T^2$ is found experimentally, the question arises as to whether this quadratic dependence is due to electron–electron

Table 1. $\nu_{ph} = \beta T^2$

Metal	Group of carriers	$10^{-7}\beta$, $(K)^{-2}\,s^{-1}$	Method	Reference	Notes
Bi	Electrons	7·7	RFSE	Gantmakher and Leonov 1968	Frequency 10^7 Hz
	Electrons	20–23	CR	Drew and Strom 1970	$(8–36)\times10^9$ and 9×10^{11} Hz
	Electrons	20–100	CR	Cheremisin *et al* 1971	$(10–35)\times10^9$ Hz
Sb	Holes	10	RFSE	Gantmakher and Dolgopolov 1971	Angle between field and long axis of ellipsoid less than 70°
	Electrons	26			
Ga	$k_f \approx 0{\cdot}01$ Å^{-1}	3	RFSE	Neighbor *et al* 1971	ν_{ph} calculated from mean free path, assuming $v = 10^8$ cm s^{-1}
Mo	Holes	2·5	RFSE	Boiko and Gasparov 1971	$1{\cdot}5 < T < 16$ K
	Electrons	2·4			$1{\cdot}5 < T < 12$ K

Table 2. $\nu_{ph} = \beta T^3$

Metal	Group of carriers	$10^{-7}\beta$, $(K)^{-3}\,s^{-1}$	Method	References	Notes
K		2·7	RFSE	Tsoi and Gantmakher 1969	Ineffectiveness of collisions over part of the orbit not taken into account
				Blaney and Parsons 1970	
Sn	4th zone	0·75	RFSE	Gantmakher and Sharvin 1965	
				Druyvestein and Smets 1971	
Pb	3rd zone	10	CR	Krasnopolin and Khaikin 1970	
	$m_c = 0{\cdot}56m_0$	$16{\cdot}4[1+(\omega/\omega_0)^3]$	CR	Goy and Castaing 1973	$0 < \omega < 4{\cdot}6\times10^{11}$ Hz; $\omega_0 = 5{\cdot}2\times10^{11}$ Hz
Ga	$m_c = 0{\cdot}9m_0$	2·7	CR	Moore 1966	
In	2nd zone, near ⟨111⟩	3·2	RFSE	Krylov and Gantmakher 1967	
		$1{\cdot}2–0{\cdot}023\chi^2$	RFSE	Snyder 1972	χ is the angle from ⟨111⟩ in the spherical cup
Cu	belly	0·3	CR	Haüssler and Welles 1966	
	$H \parallel [100]$	0·15	Sound absorption	Phua and Peverley 1971	
	neck	3	CR	Haüssler and Welles 1966	
		0·1–3·5	Surface levels	Doezema and Koch 1972	10 values at various points on the fermi surface
		0·2–2·5	RFSE	Gantmakher and Gasparov 1973	18 values averaged over various orbits

collisions, whose frequency is known to vary as $\nu_e \propto T^2$ (Ziman 1960). The following points are relevant to bismuth. Its electron fermi surfaces are elongated ellipsoids and the inequality in (14) is well satisfied for these at helium temperatures. Estimates from (40), using values of the deformation potential from independent experiments (Walther 1968), give a value $\nu_{ph}^{(theor)}$ which is even a factor of two or three larger than that observed experimentally in the RFSE.† We may conclude from this that the observed dependence $\nu_{eff}(T)$ is due to phonons, because otherwise we would have to ask why collisions with phonons were not observed. On the other hand, a number of authors note that a quadratic dependence is also observed in the temperature range 5–10 K, where the right-hand inequality in (14) no longer holds ($\hbar k_{2f} s \approx 8$ K), so that phonon scattering should already have produced a linear dependence. The assumption that $\nu_{eff} - \nu_0$ is due to phonons is also confirmed by the dependence of the coefficient of the temperature-dependent part of the electrical resistivity on carrier concentration in bismuth–antimony alloys (Fenton *et al* 1969). The observed variation $\rho - \rho_0 \propto T^2$ for the temperature dependence of the electrical resistivity of bismuth itself agrees with this assumption, because $\nu_{tr} = \nu_{ph}$ in view of (14).

A quadratic dependence of $\nu_{eff} - \nu_0$ for electrons in bismuth has also been observed in CR, but the coefficient β in these experiments was 2–3 times greater than in RFSE. We have already seen that β can increase with increasing frequency (for instance, in lead, see §4.3.4); however, this increase in bismuth begins at too low a frequency. This is clearly associated with some peculiarity of the electron spectrum in bismuth, but just what is not yet known.

6.1.2. Antimony. Here the left-hand inequality in (14) is no longer satisfied, for both hole and electron ellipsoids, and we have $k_{1f} \approx q_T \ll k_{2f}$. Antimony should therefore fall into the intermediate region between T^2 and T^3; however, as in bismuth we find that $\nu_{ph}^{(theor)} < (\nu_{eff} - \nu_0)$, which gives grounds for thinking that the measured quantity is due just to collisions with phonons.

6.1.3. Small groups in other metals. The results for gallium are very curious. As can be seen from table 2, ν_{ph} varies as T^3 for a section with large k_f (cyclotron mass $m_c = 0{\cdot}9m_0$), but for a section with $k_f \approx 0{\cdot}01$ Å^{-1}, which is four times smaller than that for antimony, ν_{ph} varies as T^2. It is very difficult here to bring in the electron–electron interaction. (In the electrical resistivity of gallium $\rho - \rho_0 \propto T^5$, since its conductivity is mainly determined by large pieces of the fermi surface.) Thus a phonon scattering frequency proportional to T^2 has already been observed for three metals with small groups of carriers. The example of gallium shows that a quadratic dependence $\nu_{ph}(T)$ probably also holds for small pieces of the fermi surfaces of other metals, where (14) is valid, and these pieces may be topologically connected to large surfaces, for instances, we may have a long narrow neck joining two surfaces.

A linear dependence $\nu_{ph}(T)$ has so far been observed only in the electrical resistivity. The fermi surfaces of all known small pockets in metals are very elongated, and in attempts to satisfy the condition in (12) by raising the temperature one finds that first, the kinetic effects themselves disappear because of the small

† In the formulae in the paper by Gantmakher and Dolgopolov (1971), where this question is also discussed, a factor of 2 is missing, compared to (39) and (40), because they took account only of the rate at which electrons leave the state $\boldsymbol{k}$. Taking account of the rate at which electrons are scattered into the state doubles the value of ν_{ph} for the same value of $\tilde{\Delta}$.

electron mean free path, and secondly, Umklapp processes to other pieces of fermi surface begin to occur from the pocket being studied, which in this case must be topologically separate. However, the variety of known fermi surfaces is continually increasing, because of the many metallic compounds, so that it is quite likely that it may be possible to find a suitable material for the observation of a linear dependence of $\nu_{ph}(T)$ for a particular electron pocket.

6.1.4. Molybdenum. A quadratic dependence of $\nu(T)$ is also observed for molybdenum, over nearly all the fermi surface. The electrical resistivity of these metals also gives $\rho - \rho_0 \sim T^2$. The 'geometrical' explanation based on (14) and (15) is clearly not applicable here. It is usually considered that the electron–electron collision frequency in transition metals is much higher than that in simple metals, and this is based on the assumption that there is a narrow d-band with a high density of states, which serves more or less as a trap for electrons. However, the fermi surface of molybdenum is well known (Boiko *et al* 1969) and by comparison with the theoretical calculations of Loucks (1965) it is clear that all pieces of the surface are seen experimentally, whilst the cyclotron resonance measurements (Herrmann 1968) show that there are no regions with high effective masses ie there is no narrow d band. Neither the fermi surface area nor the velocity distribution on the surface gives grounds for expecting it to have a larger frequency ν_e than for simple metals.

It could be suggested that the electron–electron interaction is observed in molybdenum not so much because of the high value of the frequency ν_e, but more because of the low value of the frequency ν_{ph}, as a consequence of the high Debye temperature T_D. However, this hypothesis is clearly not justified, because in copper, which also has a high Debye temperature, $\nu_{eff} - \nu_0 \propto T^3$. Thus the dependence $\nu_{eff} - \nu_0 \propto T^2$ observed for molybdenum has not yet found any consistent explanation, although it seems almost obvious that any such explanation must be based on the fact that this is a transition metal.

6.2. *Anisotropy*

The majority of the experiments quoted in tables 1 and 2 were undertaken with the aim of either determining the exponent in the dependence of $\nu_{ph}(T)$ or demonstrating the usefulness of a particular method for determining the total phonon collision frequency. However, for a number of metals—antimony, indium and especially copper—more or less systematic results for the dependence of $\nu_{ph}(\boldsymbol{k})$ are available.

6.2.1. Antimony. The dimensions of the fermi surfaces in antimony satisfy $k_f \ll K$. The scalar deformation potential $\Delta(\boldsymbol{k})$ used in (10) and (15) can then be regarded as constant on each of these surfaces. The ratio of these constants for the electron and hole surfaces is $|\Delta_{el}|/|\Delta_h| \approx 1{\cdot}5$. By using an ellipsoidal model we can draw some conclusions about the variation of ν_{ph} over the fermi surface itself. In the central region of the 'ellipsoids' ν_{ph} must vary very slowly, as does the mean value of the fermi velocity in the neighbourhood of this point. Indeed, it was not possible to observe experimentally any change in the average value of the collision frequency, even for angles as large as 70° between the field $\boldsymbol{H}$ and the ellipsoid axis. On the other hand, the change in ν_{ph} at the ends of the ellipsoids can be considerable, since $v_i \propto k_{1f}^{-1}$ along the major axes of the ellipsoids. The difference between the mean

free paths is even larger: $l_{ph} = v_i/v_{ph} \sim k_{if}^{-2}$. For example, in bismuth, where $k_{max}/k_{min} \approx 14$ for the electrons, the ratio $l_{ph}^{max}/l_{ph}^{min}$ can reach 200. This ratio in antimony is approximately 30 for electrons and 10 for holes. (In these estimates, of course, neither the anisotropy of the phonon spectrum nor the $\boldsymbol{k}$ dependence of the region of integration in (15) is taken into account.) The smallness of l_{ph}^{min} is probably the reason why it is so difficult to observe effects from extremal sections passing over the long axis of the ellipsoids.

6.2.2. Indium. It should be noted that conclusions drawn from an ellipsoidal model with a value of Δ independent of $\boldsymbol{k}$ and an isotropic phonon spectrum should be used with caution. It would seem that the frequency ν_{ph} should also be constant in indium for the spherical parts of the hole surface in the second zone, where the velocity v is practically constant in magnitude. However, according to the measurements of Snyder (1971), the frequency ν_{ph} is strongly dependent on the angle χ between the vector $\boldsymbol{k}$ and the [111] direction, and over a 15° interval it is given by the expression

$$\nu_{ph} = 10^7\,(1{\cdot}2 + 0{\cdot}023\chi^2)T^3$$

(χ is in degrees, and T in K). This means that the frequency ν_{ph} is increased approximately fivefold at the edges of this 15° region compared with its value at the centre, in the [111] direction. (The measurements were made using the RFSE from a limiting point, so that the extremal orbit was completely contained within the spherical cup for all directions of the field.) It seems most natural to suppose that such a rapid dependence is associated with anisotropy of the phonon spectrum but this suggestion has not been numerically analysed.

6.2.3. Copper. The most detailed measurements of the electron–phonon collision frequency have been made for copper. These measurements are important from two points of view.

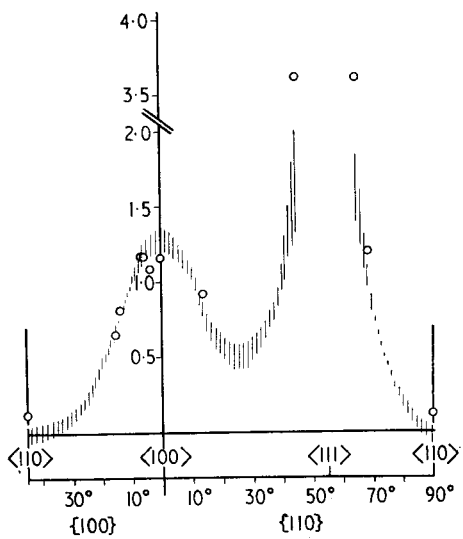

Figure 22. Dependence $\nu_{ph}(\boldsymbol{k})$ for the fermi surface of copper in the (100) and (110) planes. The open circles are from measurements by Doezema and Koch (1972), using surface levels; the vertical lines are results from Gantmakher and Gasparov (1973), obtained from RFSE.

First, copper is so far the only metal for which the function $\nu_{ph}(\boldsymbol{k})$ has been measured over the whole fermi surface. The measurements for copper are all the more valuable because a theoretical calculation of $\nu_{ph}(\boldsymbol{k})$ was made by Novak (1972). The results of measurements by Doezema and Koch (1972) from the shape of resonance lines due to surface levels are shown by points in figure 22, whilst the vertical bars show the results obtained by Gantmakher and Gasparov from the RFSE. These are calculated from measured values of $\langle \nu_{ph} \rangle$ (see equation (52)) for various extremal orbits, the network of which gave sufficiently close coverage over the whole fermi surface. (For the mathematical details see the above reference, and also Springford (1971) and Bosacchi *et al* (1972).)

The value of the experiments on copper is also that all the methods discussed here have been applied. The agreement of the results can be regarded as experimental confirmation of the correctness of the concepts used.

Acknowledgments

The author is grateful to Y B Levinson, E A Kaner, R N Gurzhi and V T Dolgopolov for valuable discussions and important comments.

References

References to English translations of journals in Russian are given in parentheses after the reference to the Russian original.

AKHIEZER A J 1938 *ZhETF* **8** 1330–9
AZBEL' M JA and KANER E A 1958 *J. Phys. Chem. Solids* **6** 113–35
BLANEY T G and PARSONS D 1970 *J. Phys. C: Solid St. Phys.* **3** 126–37
BOIKO V V and GASPAROV V A 1971 *Metallofizika* (Kiev: Naukova Dumka) **37** 11–5
BOIKO V V, GASPAROV V A and GVERDTSITELI I G 1969 *ZhETF* **56** 489–500 (*Sov. Phys.—JETP* **29** 267–73)
BOSACCKI B, KETTERSON J B and WINDMILLER L R 1972 *Phys. Rev.* B **5** 3816–8
CAPLIN A D and RIZZUTO C 1971 *Austral. J. Phys.* **24** 309–16
CHAMBERS R G 1965 *Proc. Phys. Soc.* **86** 305–8
CHEREMISIN S M 1972 *ZhETF Pis'ma* **16** 186–90 (*Sov. Phys.—JETP Lett.* **16** 131–34)
CHEREMISIN S M, EDELMAN V S and KHAIKIN M S 1971 *ZhETF* **61** 1112–19 (*Sov. Phys.—JETP* **34** 594–7)
DEATON B C 1965 *Phys. Rev.* **140** A2051–5
DEATON B C and GAVENDA J D 1964 *Phys. Rev.* A **136** 1096–101
DOEZMA R E and KOCH J F 1972 *Phys. Rev.* B **6** 2071–77
DREW H D 1972 *Phys. Rev.* B **5** 360–6
DREW H D and STROM U 1970 *Phys. Rev. Lett.* **25** 1755–8
DRUYVESTEIN W F and SMETS A J 1970 *J. Low Temp. Phys.* **2** 619–30
EKIN J W and MAXFIELD B W 1971 *Phys. Rev.* B **4** 4215–25
ENGELSBERG S and SIMPSON G 1970 *Phys. Rev.* B **2** 1657–65
FENTON E W, JAN J-P, KARLSSON A and SINGLER R 1969 *Phys. Rev.* **184** 663–7
GAIDUKOV JU P and KADLECOVA JA 1970 *ZhETF* **59** 700–11 (*Sov. Phys.—JETP* **32** 382–8)
GANTMAKHER V F 1967 *Progr. in Low Temp. Phys.* **5** ed C J Gorter (Amsterdam: North-Holland) pp181–234
—— 1972 *ZhETF Pis'ma* **16** 256–9 (*Sov. Phys.—JETP Lett.* **16** 180–82)
GANTMAKHER V F and DOLGOPOLOV V T 1971 *ZhETF* **60** 2260–8 (*Sov. Phys.—JETP* **33** 1215–9)
GANTMAKHER V F and GASPAROV V A 1972 *ZhETF* **64** 1712–23 (*Sov. Phys.—JETP* **37**)
GANTMAKHER V F and LEONOV JU S 1968 *ZhETF Pis'ma* **8** 264–7 (*Sov. Phys.—JETP Lett.* **8** 162–4)
GANTMAKHER V F and SHARVIN JU V 1965 *ZhETF* **48** 1077–80 (*Sov. Phys.—JETP* **21** 720–2)

GOLD A V 1969 *Solid State Physics* vol 1 *Electrons in Metals* eds J F Cochran and R R Haering (New York: Gordon and Breach) pp39–126
GOY P and CASTAING B 1972 *Phys. Rev.* B **7** 4409–524
GOY P and WEISBUCH G 1969 *Phys. Kondens. Materie* **9** 200–7
GURZHI R N 1968 *Usp. Fiz. Nauk* **94** 589–718 (*Sov. Phys.—Uspekhi* **11** 255–70)
GURZHI R N and KOPELOVICH A J 1971 *ZhETF* **61** 2514–29 (*Sov. Phys.—JETP* **34** 1345–52)
HABERLAND P H and SHIFFMAN C A 1967 *Phys. Rev. Lett.* **19** 1337–41
HAÜSSLER P and WELLES S J 1966 *Phys. Rev.* **152** 675–82
HEINE V 1957 *Phys. Rev.* **107** 431–7
HERRMANN R 1968 *Phys. Stat. Sol.* **25** 427–35
KAGAN JU and ZHERNOV A P 1971 *ZhETF* **60** 1832–44 (*Sov. Phys.—JETP* **33** 990–6)
KAMGAR A, HENNINGSEN J O and KOCH J F 1972 *Phys. Rev.* B **6** 342–7
KANER E A and AZBEL'M JA 1957 *ZhETF* **33** 1461–71 (*Sov. Phys.—JETP* **6** 1126–34)
KANER E A and GANTMAKHER V F 1968 *Usp. Fiz. Nauk.* **94** 193–241 (*Sov. Phys.—Uspekhi* **11** 81–106)
KANER E A, PESCHANSKII V G and PRIVOROTSKII J A 1961 *ZhETF* **40** 214–26 (*Sov. Phys.—JETP* **13** 147–55)
KHAIKIN M S 1968 *Usp. Fiz. Nauk* **96** 409–40 (*Sov. Phys.—Uspekhi* **11** 785–801)
KLEMENS P G and JACKSON J L 1964 *Physica* **30** 2031–40
KOCH J F and DOEZEMA R E 1970 *Phys. Rev. Lett.* **24** 507–10
KRASNOPOLIN J JA and KHAIKIN M S 1970 *ZhETF Pis'ma* **12** 76–9 (*Sov. Phys.—JETP Lett.* **12** 54–6)
KRYLOV I P and GANTMAKHER V F 1966 *ZhETF* **51** 740–5 (*Sov. Phys.—JETP* **24** 492–5)
LOUCKS T L 1965 *Phys. Rev.* A **139** 1181–8
MACDONALD D K C 1956 *Handbuch der Phys.* **14** ed S Flügge (Berlin: Springer-Verlag) pp137–97
MOORE T W 1966 *Phys. Rev. Lett.* **16** 581–3
MYERS A, PORTER S G and THOMPSON R S 1972 *J. Phys. F: Metal Phys.* **2** 24–37
NABEREZHNYKH V P and TSYMBAL L T 1967 *ZhETF Pis'ma* **5** 319–22 (*Sov. Phys.—JETP Lett.* **5** 263–5)
NABEREZHNYKH V P, TSYMBAL L T and PURCHINSKII M S 1971 *Phys. Stat. Sol.* B **44** 845–8
NEE T W and PRANGE R E 1967 *Phys. Lett.* **25** A 582–3
NEIGHBOR J E, SHIFFMAN C A, CHATJIGIANNIS D G and JACOBSEN S P 1971 *Phys. Rev. Lett.* **27** 929–32
NOVAK D 1972 *Phys. Rev.* B **6** 3691–99
PALIN C J 1972 *Proc. R. Soc.* A **329** 17–34
PEIERLS R E 1955 *Quantum Theory of Solids* (Oxford: Clarendon Press)
PHUA M S and PEVERLEY J R 1971 *Phys. Rev.* B **3** 3115–20
PIPPARD A B 1960 *Rep. Prog. Phys.* **23** 176–266
—— 1964 *Proc. R. Soc.* A **282** 464–84
—— 1968 *Proc. R. Soc.* A **305** 291–318
POULSEN R G and DATARS W R 1970 *Sol. St. Commun.* **8** 1969–73
SHARVIN JU V and BOGATINA N J 1969 *ZhETF* **56** 772–9 (*Sov. Phys.—JETP* **29** 419–23)
SNYDER P M 1971 *J. Phys. F: Metal Phys.* **1** 363–72
SPRINGFORD M 1971 *Adv. Phys.* **20** 493–550
STARK R W, TRIVISONNO J and SCHWARZ R E 1971 *Phys Rev.* B **3** 2465–76
TSOI V S 1969 *Fiz. Metall.* **28** 565–7 (*Sov. Phys.—Phys. Metal. Metallogr.* **28**)
TSOI V S and GANTMAKHER V F 1969 *ZhETF* **56** 1232–41 (*Sov. Phys.—JETP* **29** 663–8)
WALTHER K 1968 *Phys. Rev.* **174** 782–90
YOUNG R A 1968 *Phys. Rev.* **175** 813–23
ZIMAN J M 1960 *Electrons and Phonons* (Oxford: Clarendon Press)
—— 1964 *Principles of the Theory of Solids* (London: Cambridge University Press)
—— 1969 (ed) *The Physics of Metals—1 Electrons* (London: Cambridge University Press) pp1–249